



Natural Resources
Canada

Ressources naturelles
Canada

**GEOLOGICAL SURVEY OF CANADA
OPEN FILE 8746**

**Analyzing spatial patterns of thermal alteration in the Stikine
and Wrangell Terranes of the Canadian Cordillera using
the conodont color alteration index (CAI) to identify
hot spots and cold spots**

J. Z. X. Lei, M. L. Golding, and J. M. Husson

2020

Canada 



**GEOLOGICAL SURVEY OF CANADA
OPEN FILE 8746**

**Analyzing spatial patterns of thermal alteration in the
Stikine and Wrangell Terranes of the Canadian Cordillera
using the conodont color alteration index (CAI) to identify
hot spots and cold spots**

J. Z. X. Lei¹, M. L. Golding², and J. M. Husson¹

¹School of Earth and Ocean Sciences, University of Victoria, 3800 Finnerty Road, Bob Wright Centre A405, Victoria, British Columbia

²Geological Survey of Canada, 605 Robson Street, Vancouver, British Columbia

2020

© Her Majesty the Queen in Right of Canada, as represented by the Minister of Natural Resources, 2020

Information contained in this publication or product may be reproduced, in part or in whole, and by any means, for personal or public non-commercial purposes, without charge or further permission, unless otherwise specified.

You are asked to:

- exercise due diligence in ensuring the accuracy of the materials reproduced;
 - indicate the complete title of the materials reproduced, and the name of the author organization; and
 - indicate that the reproduction is a copy of an official work that is published by Natural Resources Canada (NRCan) and that the reproduction has not been produced in affiliation with, or with the endorsement of, NRCan.
- Commercial reproduction and distribution is prohibited except with written permission from NRCan. For more information, contact NRCan at nrcan.copyrightdroitdauteur.nrcan@canada.ca.

Permanent link: <https://doi.org/10.4095/327243>

This publication is available for free download through GEOSCAN (<https://geoscan.nrcan.gc.ca/>).

Recommended citation

Lei, J. Z. X., Golding, M. L., and Husson, J. M., 2020. Analyzing spatial patterns of thermal alteration in the Stikine and Wrangell Terranes of the Canadian Cordillera using the conodont color alteration index (CAI) to identify hot spots and cold spots; Geological Survey of Canada, Open File 8746, 1 .zip file. <https://doi.org/10.4095/327243>

Publications in this series have not been edited; they are released as submitted by the author.

ABSTRACT

Spatial analysis has been conducted on CAI data from archival conodont collections across the Canadian Cordillera of British Columbia and Yukon, creating thermal alteration maps with Kriging interpolation surfaces and Getis-Ord G_i^* statistical hot spots. Major hot spots include the southeast corner of British Columbia, the central coast of British Columbia, southern Vancouver Island, and most of the British Columbia - Yukon border. Major cold spots include the northeast quadrant of British Columbia, the northern tip of Vancouver Island, and central Haida Gwaii. Hot spots on Vancouver Island generally correlate with the prevalence of intrusive units nearby; however, the largest hot spot coincides with a southern region unique on the island for having significant outcroppings of Permian limestone, which is more heavily altered than the Triassic limestones commonly sampled for conodonts further north on the island. Comparison of locations where paleoenvironmental studies have utilized $\delta^{13}\text{C}$, both near the British Columbia - Yukon border, as well as at the far north of Vancouver Island, demonstrates that stratigraphic sections which preserves a primary $\delta^{13}\text{C}$ signal tends to be situated closer to the center of a thermal alteration cold spot than sections that do not. Beyond the select examples discussed in this study, the broader analysis has potential applications in a wide variety of research, from Cordilleran tectonics to preliminary hydrocarbon exploration.

INTRODUCTION

Conodont microfossils have been used extensively in both academic and industrial settings to constrain the age of marine sedimentary rocks. This utility is due to a combination of many factors including high preservation potential, highly prolific communities, typically cosmopolitan distributions, and rapid evolutionary turnover. In addition to their use in biostratigraphy, the colour of conodont specimens can be used to estimate maximum burial temperature. This semi-quantitative approach is referred to as the conodont Color Alteration Index (CAI; Epstein et al., 1977; Rejebian et al., 1987). The present study conducts spatial analysis on CAI data extracted from the extensive Geological Survey of Canada conodont collections sampled across the Canadian Cordillera, for the purpose of creating a thermal alteration statistical hot spot map. This tool has great potential for supporting a broad range of research, from tectonic reconstruction to hydrocarbon exploration. Focusing on statistical cold spots of thermal alteration as opposed to hot spots could also assist in the selection of localities for paleoenvironmental studies that utilize proxies sensitive to thermal alteration such as $\delta^{13}\text{C}$ records. This analysis is conducted for the entire Canadian Cordillera of British Columbia and Yukon, and the ArcGIS shapefiles produced are included with the publication. Specific spatial patterns within the Stikine and Wrangell terranes have been identified for more detailed discussion.

BACKGROUND

The Canadian Cordillera

Spanning from the Canadian Rockies to the Pacific coastline, the Canadian Cordillera refers to a large zone of deformation resulting from accretionary orogenesis (Figure 1; Monger, 1997). It consists of an amalgamation of crustal terranes with various stratigraphic and tectonic histories (Monger and Ross, 1971). The relationships between these terranes, and their relative positions throughout the late Paleozoic and Mesozoic prior to accretion to the North American margin, are still poorly constrained and contentious. The terranes have been interpreted as fragments of continental crust, oceanic crust, or volcanic island arcs (Colpron and Nelson, 2011). Faunal distributions, paleomagnetism, detrital zircon geochronology, and crustal geochemistry have been used to constrain the movements of these terranes through geologic time, and many

studies have recognized considerable latitudinal and longitudinal displacement prior to accretion (e.g. Monger and Ross, 1971; Jones et al., 1977; Mihalynuk et al., 1994; Belasky et al., 2002; Johnston, 2008; Kent and Irving, 2010; Beranek and Mortensen, 2011). Because of this complex tectonic history, thermal alteration of various origins is pervasive throughout the region.

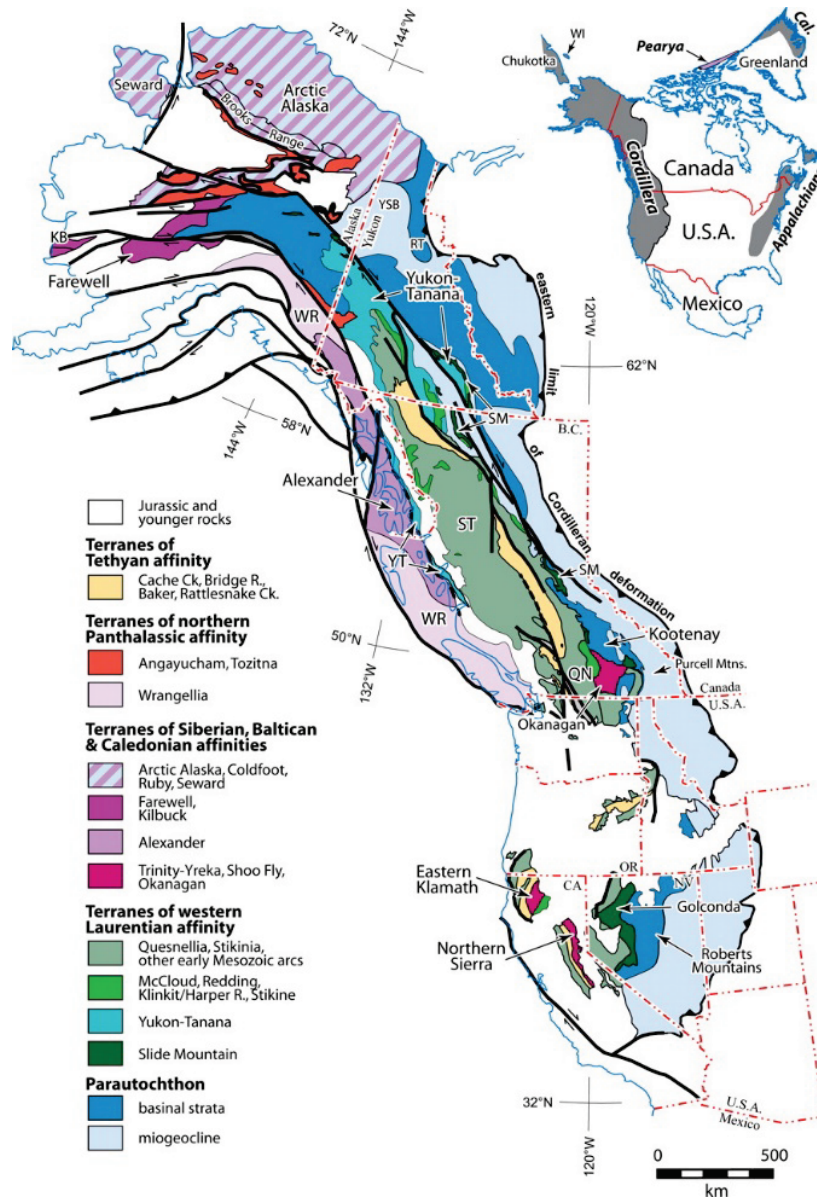


Figure 1: Terrane map of the North American Cordillera. From Colpron and Nelson (2009).

The Stikine Terrane is an extensive island arc terrane within the Intermontane Belt located in British Columbia and southern Yukon (Figure 1; Monger, 1977). It is characterized by late Paleozoic volcanic rocks of island arc origin, overlain by interbedded Triassic through Early

Jurassic marine carbonate, siliciclastic, and volcanic rocks (Monger, 1977). The The Wrangell Terrane is an oceanic terrane within the Insular Belt located on Vancouver Island, Haida Gwaii, and throughout southern Alaska (Figure 1; Jones et al., 1977). It is characterized by Middle to Late Triassic tholeiitic volcanic rocks overlain by Late Triassic marine carbonate and siliciclastic rocks (Jones et al., 1977).

Conodont Color Alteration Index (CAI)

CAI is a semi-quantitative property of conodonts that makes these microfossils useful for geothermometry (Epstein et al., 1977; Rejebian et al., 1987). As a conodont element undergoes burial and heating, the organic material within it carbonizes in a reaction that visibly and non-reversibly changes the colour of the specimen. From pale translucent yellow, the element becomes incrementally darker until it is black, and eventually it will turn white and then clear as the organic matter is lost (Epstein et al., 1977; Rejebian et al., 1987). Different shades of colour are assigned CAI values, each of which corresponds to a range of maximum temperatures (Epstein et al., 1977). The variation in conodont colouration and the corresponding maximum temperature ranges are displayed in Figure 2.







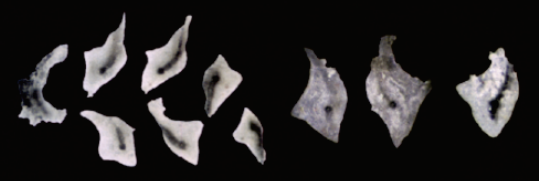

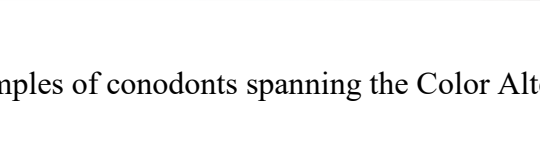
CAI	Naturally altered conodonts from field samples (Rheinisches Schiefergebirge and Montagne Noire)	Temperature range
1		<50°-80°
2		60°-140°
3		110°-200°
4		190°-300°
5		300° - 480°
6		360° - 550°
CAI	Contact metamorphosed and/or hydrothermally altered conodonts (Rheinisches Schiefergebirge and Montagne Noire)	Temperature range
6.5		440° - 610°
7		490° - 720°
		>600°

Figure 2: Compiled examples of conodonts spanning the Color Alteration Index. From Königshof (2003).

Previous Studies

Several studies across Europe have used the geographic distribution of CAI from conodont collections to determine metamorphic zonation on a regional scale (Gawlick et al., 1994; Wiederer et al., 2002). On a larger scale, the United States Geological Survey has created CAI maps of the southwestern Basin and Range Province for the primary purpose of assessing hydrocarbon thermal maturity, largely encompassing Nevada, Utah, and Arizona (Harris et al., 1980; Wardlaw and Harris, 1984). Similarly, Legall et al. (1981) used CAI distribution to assess hydrocarbon potential in Southern Ontario and Southern Quebec, as did Orchard and Forster (1991) for Haida Gwaii, and MacNaughton et al. (2008) for parts of the Mackenzie and Selwyn mountains. Read et al. (1991a; 1991b) created a metamorphic map of the Canadian Cordillera using organic maturation from a combination of vitrinite reflectance, and CAI from conodont collections made prior to 1986 (Figure 3). The present study includes the CAI dataset used by Read et al. (1991a; 1991b), as well as conodont collections made between 1986 and 2019. None of these prior studies have utilized GIS spatial analysis, and the more quantitative approach of the present study results in greater statistical rigor than has been previously possible.

MATERIALS AND METHODS

Conodont collections data were retrieved from the paleontological database of the Geological Survey of Canada Pacific office in Vancouver. The data used in this study derives from collections made spanning the early 1970s to 2019, and totals approximately 15 000 datapoints (Figure 4). The dataset was trimmed to only include collections with associated CAI values, and with GPS coordinates falling within the Canadian Cordillera of British Columbia, Yukon, and adjacent portions of Alaska. This results in a total of 1687 datapoints for maximum CAI, and 2155 datapoints for minimum CAI. The lithology associated with the original conodont collections is predominantly carbonate, but also includes chert and argillite samples.

ArcGIS ArcMap™ 10.6.1 software was used for all spatial analysis and map creation. The Kriging process was chosen to create the interpolation surfaces due to its versatility in correcting for datasets with clustering. Due to the utility of conodonts in biostratigraphy, collections are typically highly clustered in localities with significant portions of marine sedimentary strata exposed, and also in critical age intervals within these stratigraphic sections. The Ordinary Kriging process was used, as other processes factor in known overriding trends or directional drift, neither of which are expected within this dataset (Scheeres, 2016). Three data groups were isolated with geographic limitations: all data; only datapoints within the Stikine Terrane; and only datapoints within the Wrangell Terrane. Each of these were analyzed with minimum and maximum CAI values, for a total of six individual interpolation surfaces. The Stikine and Wrangell terranes were analyzed in isolation in order to see if CAI trends in a terrane arrange independently of each other, which would result in isolated terrane trends differing from when all datapoints are used. Both these terranes host a large number of datapoints that cover a wide range of CAI values and geographic area, therefore providing ideal test cases. Figure 4 shows the distribution of these two terranes in the Canadian Cordillera. Optimizing the model showed the data was fit best by a stable semi-variogram, and this remained true for all six interpolation surfaces. A cell size of 5000 meters was used for each interpolation surface, which was sufficient to clearly display the targeted spatial patterns whilst remaining fast to compute. All datasets fit the model well, as seen by a mean standardized value close to zero, a standardized root-mean-square close to one, and an average standard error close to the standardized root-mean-square (Scheeres, 2016); refer to appendix for these statistics.

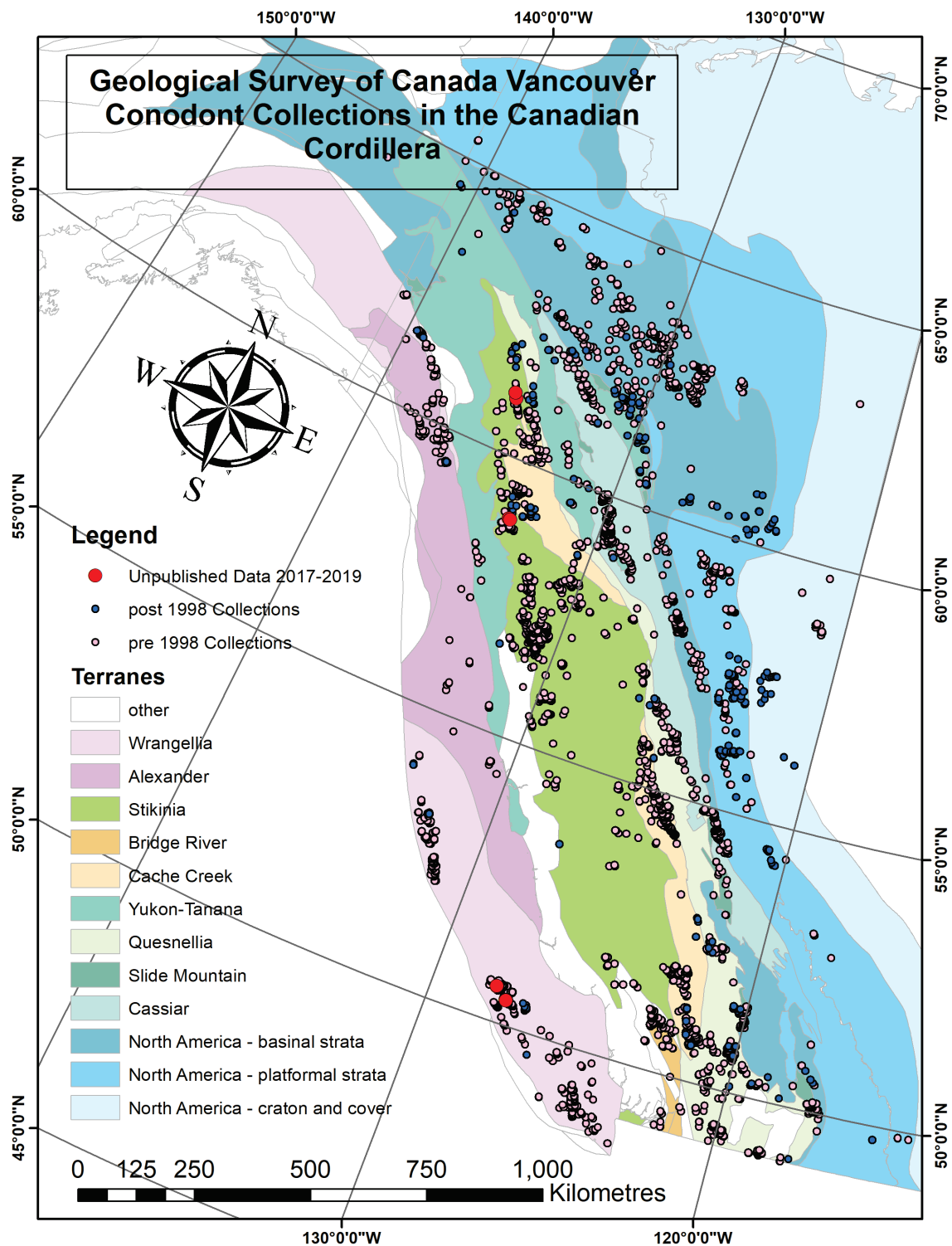


Figure 4: All collections datapoints after trimming, overlain on Cordillera terranes map modified from Colpron et al. (2007), and Nelson and Colpron (2007).

Getis-Ord G_i^* statistical hot spot analysis was conducted corresponding to each interpolation surface individually. This assigns a confidence value (99%, 95%, 90%, not significant) to each datapoint as a hot spot compared to neighbouring datapoints, complementing the qualitative spatial patterns visible in the interpolation surfaces (esri, n.d.). A fixed Euclidean threshold distance of 20 kilometers was used, as it approximates the lower end of targeted hot spot spacing seen in the interpolation surfaces. In the context of this study, hot spots indicate spatial clusters of higher than surrounding CAI values, corresponding to regions of greater thermal alteration. Cold spots correspond to regions of lesser thermal alteration.

RESULTS

From the interpolation surfaces, background CAI values across the Canadian Cordillera are moderately high at approximately 4 to 5 (Figure 5; Figure 6). Regions with thermal alteration hot spots (local maxima) include the southeast corner of British Columbia, the central coast of British Columbia, southern Vancouver Island, and most of the British Columbia - Yukon border (Figure 5; Figure 6). Regions with thermal alteration cold spots (local minima) include the northeast quadrant of British Columbia, the northern tip of Vancouver Island, and central Haida Gwaii (Figure 5; Figure 6). The broader trends of Figure 5 and Figure 6 will not be further explored by this study, as interpretations at that scale would require much greater amounts analysis and discussion.

These interpolation surfaces remain consistent with data exclusion. Individual interpolation surfaces were created for the Stikine and Wrangell terranes using only the data points that fall within each; this produced hot spot distributions very similar to that of the interpolations made using all data (Figure 5 through Figure 10). Using maximum or minimum CAI values shifts the overall values of the interpolation surfaces up and down respectively, but the location and extent of hot spots remain fixed, as assessed visually (Figure 5 through Figure 10).

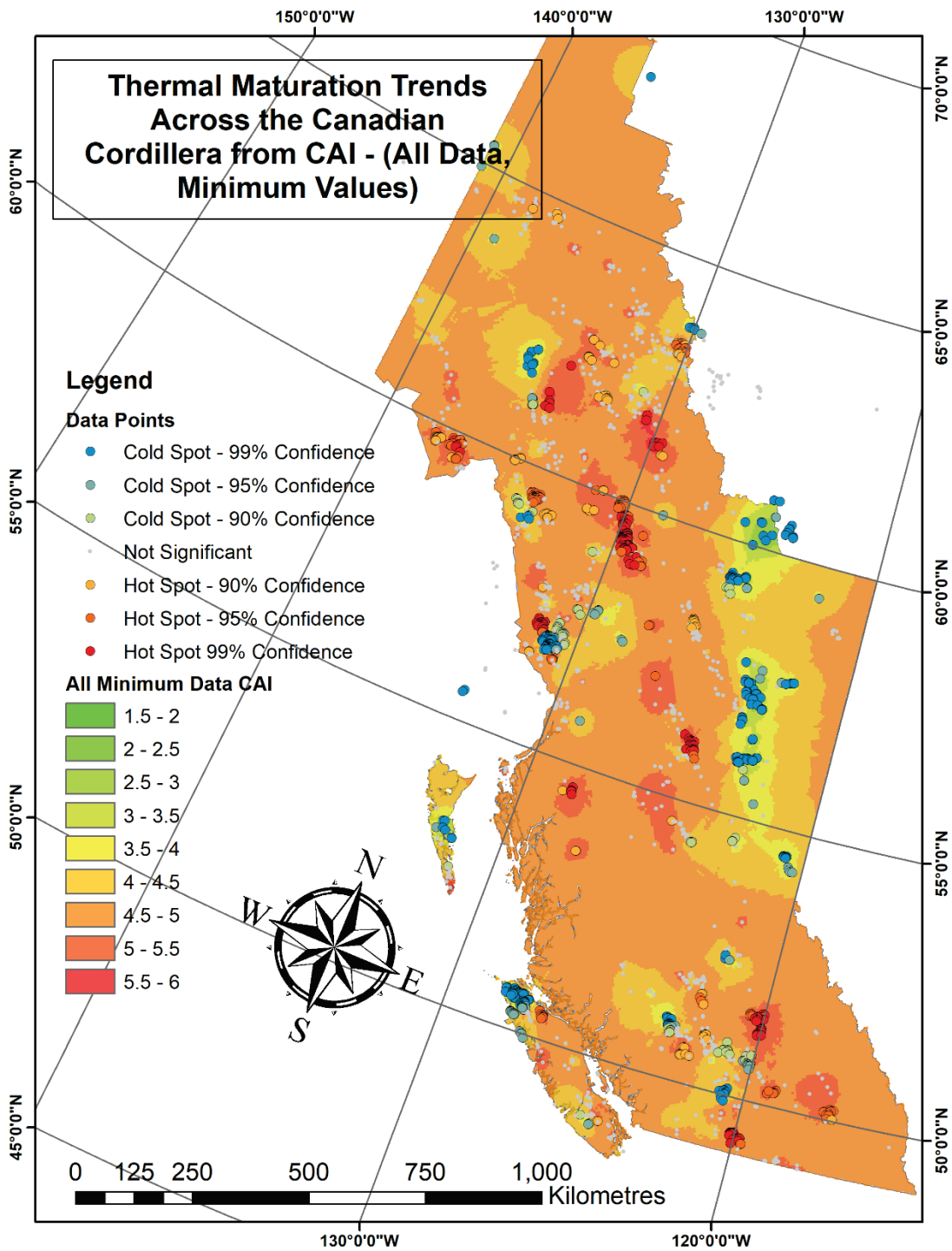


Figure 5: Thermal maturation trends across the Canadian Cordillera of British Columbia and Yukon from CAI. All data included; minimum values.

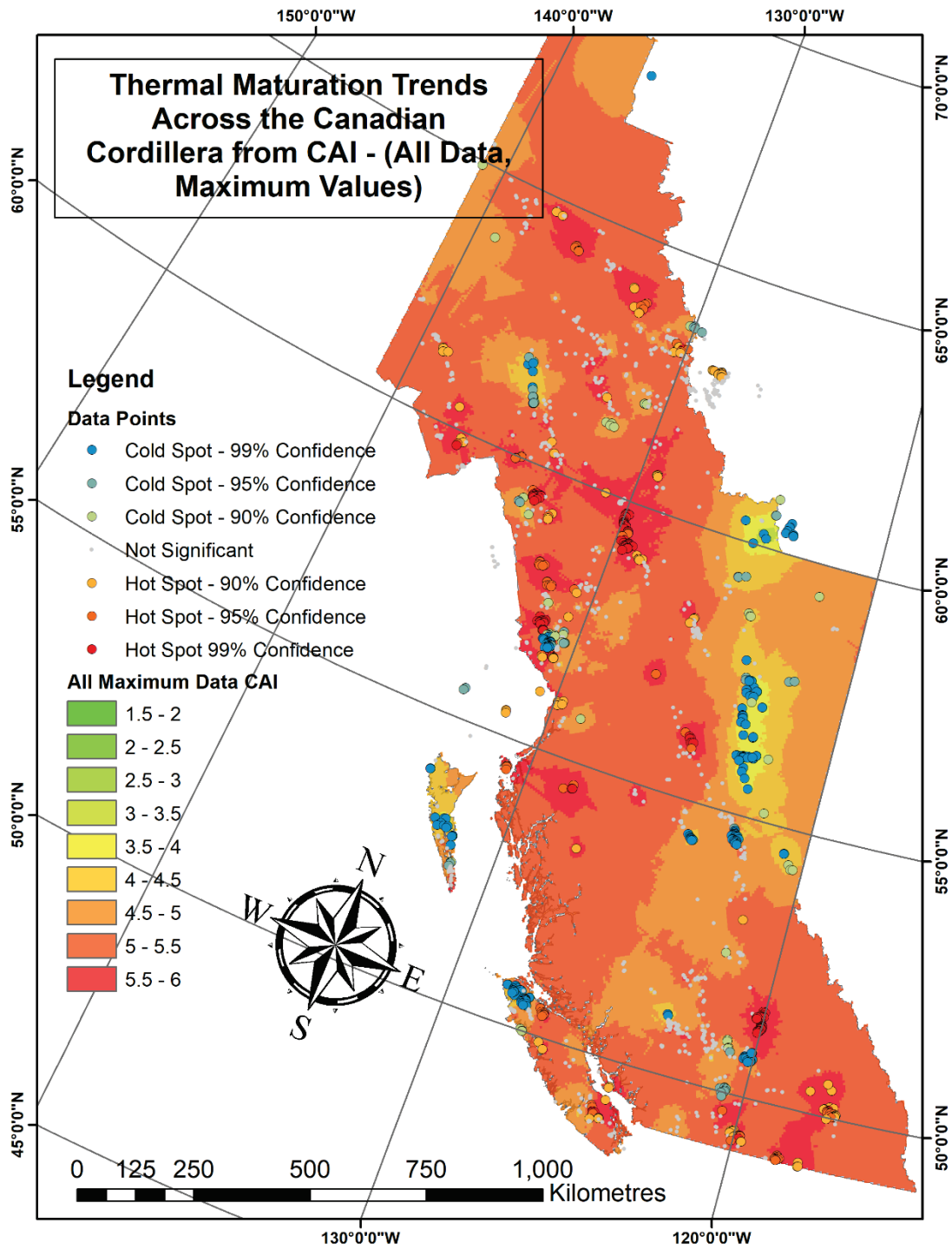


Figure 6: Thermal maturation trends across the Canadian Cordillera of British Columbia and Yukon from CAI. All data included; maximum values.

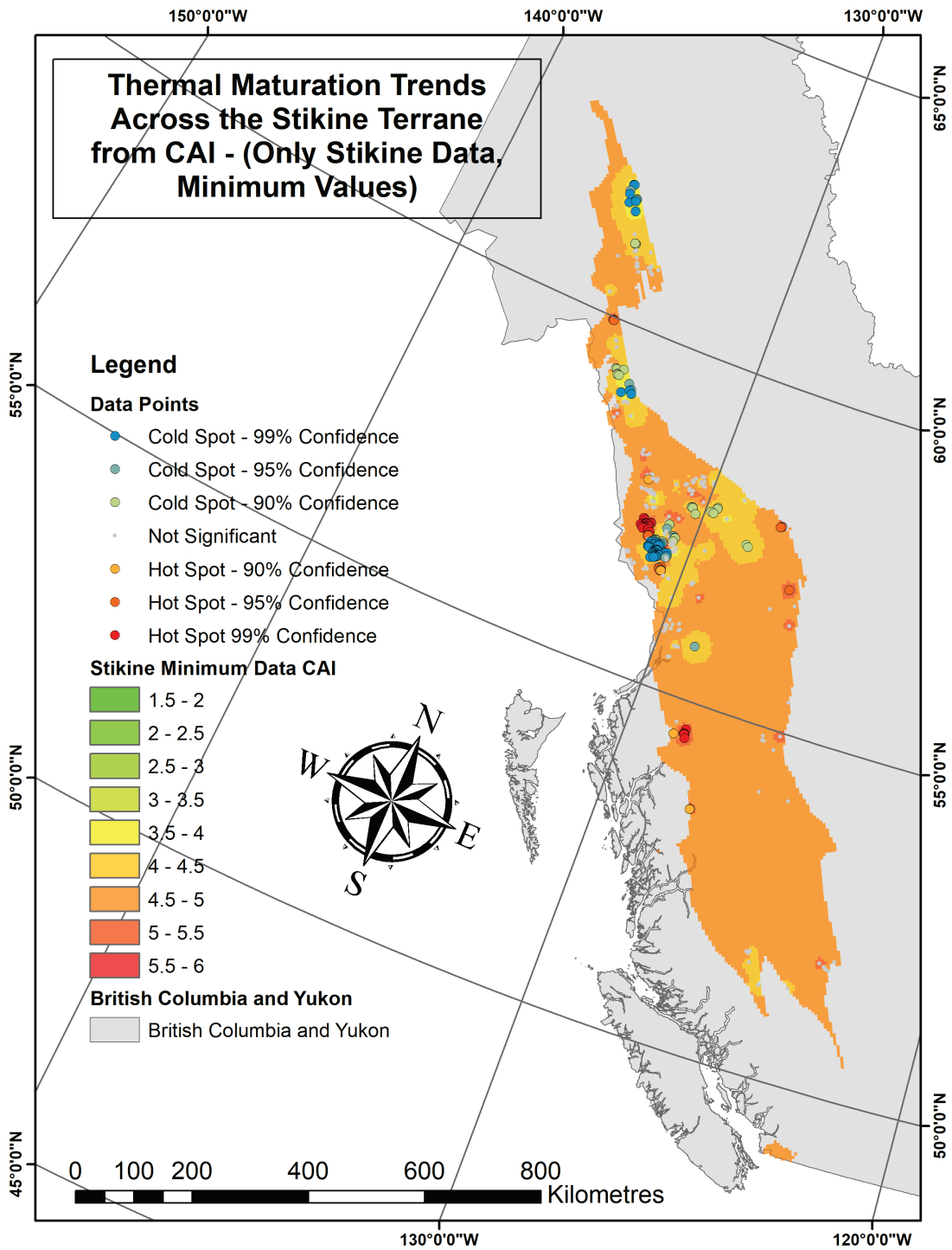


Figure 7: Thermal maturation trends across the Stikine Terrane from CAI. Only Stikine Terrane data included; minimum values.

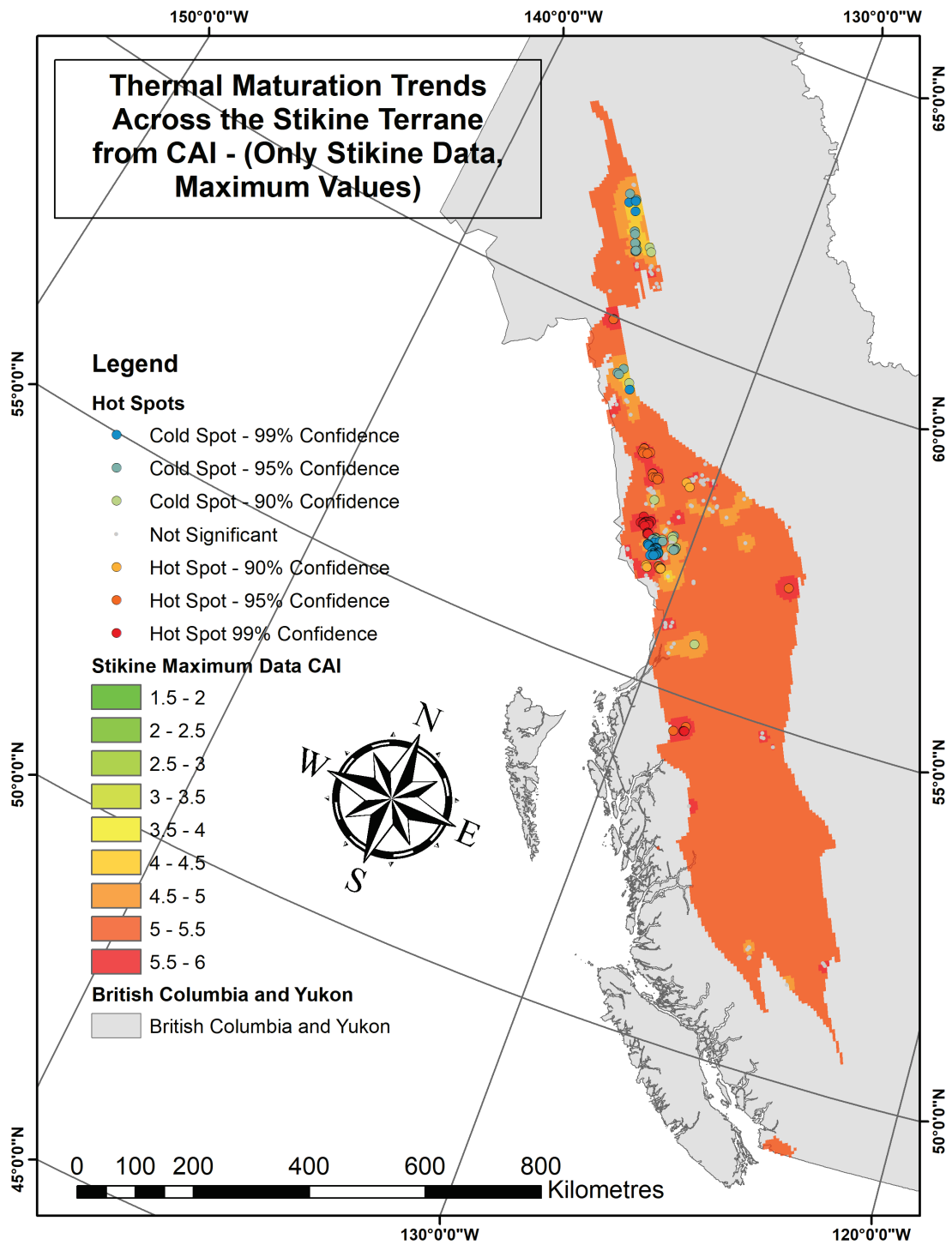


Figure 8: Thermal maturation trends across the Stikine Terrane from CAI. Only Stikine Terrane data included; maximum values.

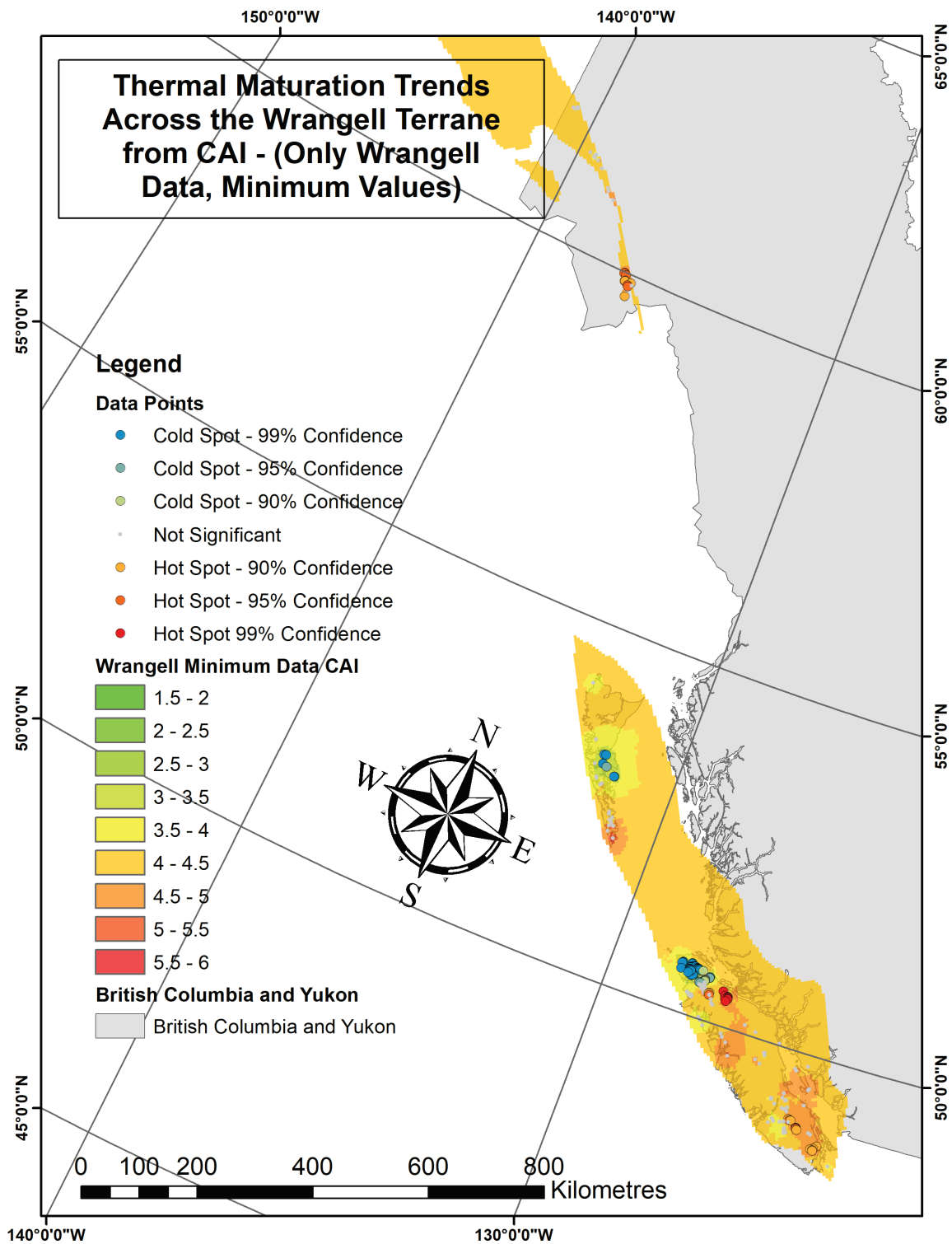


Figure 9: Thermal maturation trends across the Wrangell Terrane from CAI. Only Wrangell Terrane data included; minimum values.

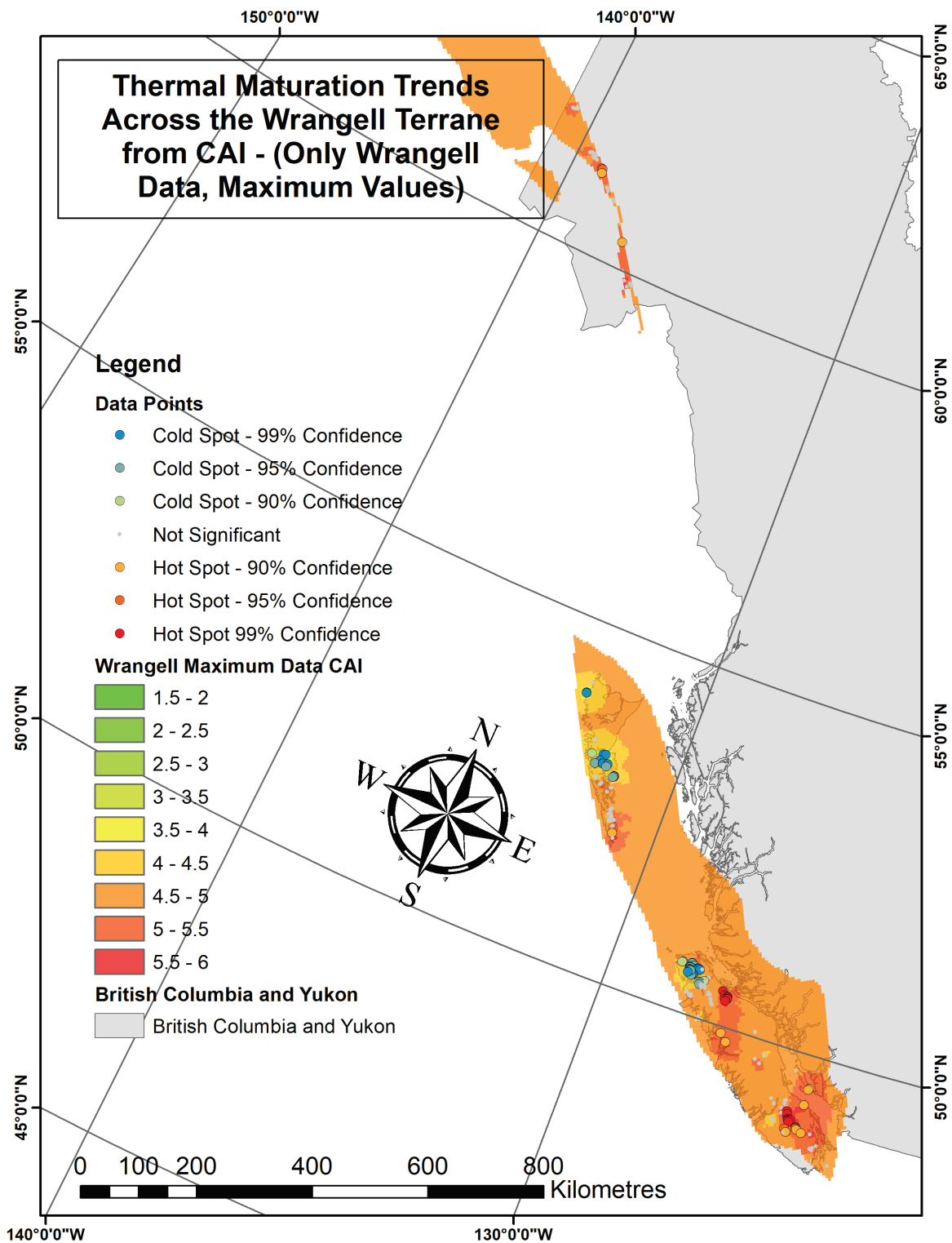


Figure 10: Thermal maturation trends across the Wrangell Terrane from CAI. Only Wrangell Terrane data included; maximum values.

DISCUSSION

Interpretation of broader thermal alteration trends across the Canadian Cordillera are beyond the scope of this study, but the following select examples are presented to demonstrate the utility of this analysis in vastly different applications. The entirety of the following discussion is based on the ‘all data’ dataset, as shown in Figure 5 and Figure 6.

Thermal Maturity of Vancouver Island

Vancouver Island displays three hot spots circled in purple, and a single cold spot circled in blue (Figure 11; Figure 12); the central hot spot is evidently less statistically strong, as it becomes not significant when using the minimum CAI dataset. The central and northern hot spots occur in the Late Triassic limestone units of the Vancouver Group, namely the Quatsino Formation, and to a lesser extent the mixed carbonate-siliciclastic-volcaniclastic Parsons Bay Formation (Figure 13; Carlisle and Suzuki, 1974; Muller, 1977; Massey and Friday, 1987). The hot spots coincide with intrusions of the younger, Jurassic Bonanza arc, which includes the Island Plutonic Suite and the Westcoast Crystalline Complex (DeBari et al., 1999; D’Souza et al., 2015). Perplexingly, there are significant areas of Island Plutonic Suite outcropping on the northern tip of Vancouver Island, proximal to a large thermal alteration cold spot (Figure 14). These intrusive units may be far more fragmented there than the current mapping would suggest, as the main body of the pluton seems to be further south, and diminishing northward; a large arm of Island Plutonic Suite reaches out from the main southern body and extends to the northern hot spot (Figure 14). Erupted volcanic units associated with Bonanza arc magmatism have been generally mapped as the Bonanza Group, and being extrusive, are not likely to have been a significant source of thermal alteration (Figure 14). These unit relationships are reflected in the Read et al. (1991a; 1991b) metamorphic map, as the zeolite/prehnite-pumpellyite facies that dominates the northern portion of Vancouver Island is variably intermixed with a post-metamorphic intrusive unit (Figure 3).

The southern hot spot occurs in the older, Permian limestone of the Buttle Lake Formation (Figure 13; Carlisle and Suzuki, 1974; Muller, 1977). The Buttle Lake Formation is intruded by the Mount Hall Gabbro, an informal unit name used to describe the mafic dikes and sills that are coeval and likely feeders to the extensive Triassic Karmutsen Formation (Figure 15;

Carlisle and Suzuki, 1974; Muller, 1977; Massey and Friday, 1987). The Buttle Lake Formation limestone has also been thermally altered by intrusions of the Jurassic Island Plutonic Suite. On Vancouver Island, the Buttle Lake Formation and Mount Hall Gabbro are uniquely well exposed in the southern part of the island. It is reasonable that the Buttle Lake Formation would be generally more thermally altered than the younger Triassic limestone, and this is supported by the large area spanned by the southern hotspot, which is also statistically the most significant of the hotspots when using maximum CAI (Figure 12). On the Read et al. (1991a; 1991b) map, this area has large exposures of chlorite zone greenschist facies rock, confirming that this southern portion of Vancouver Island is of higher metamorphic grade than the northernmost portion (Figure 3).

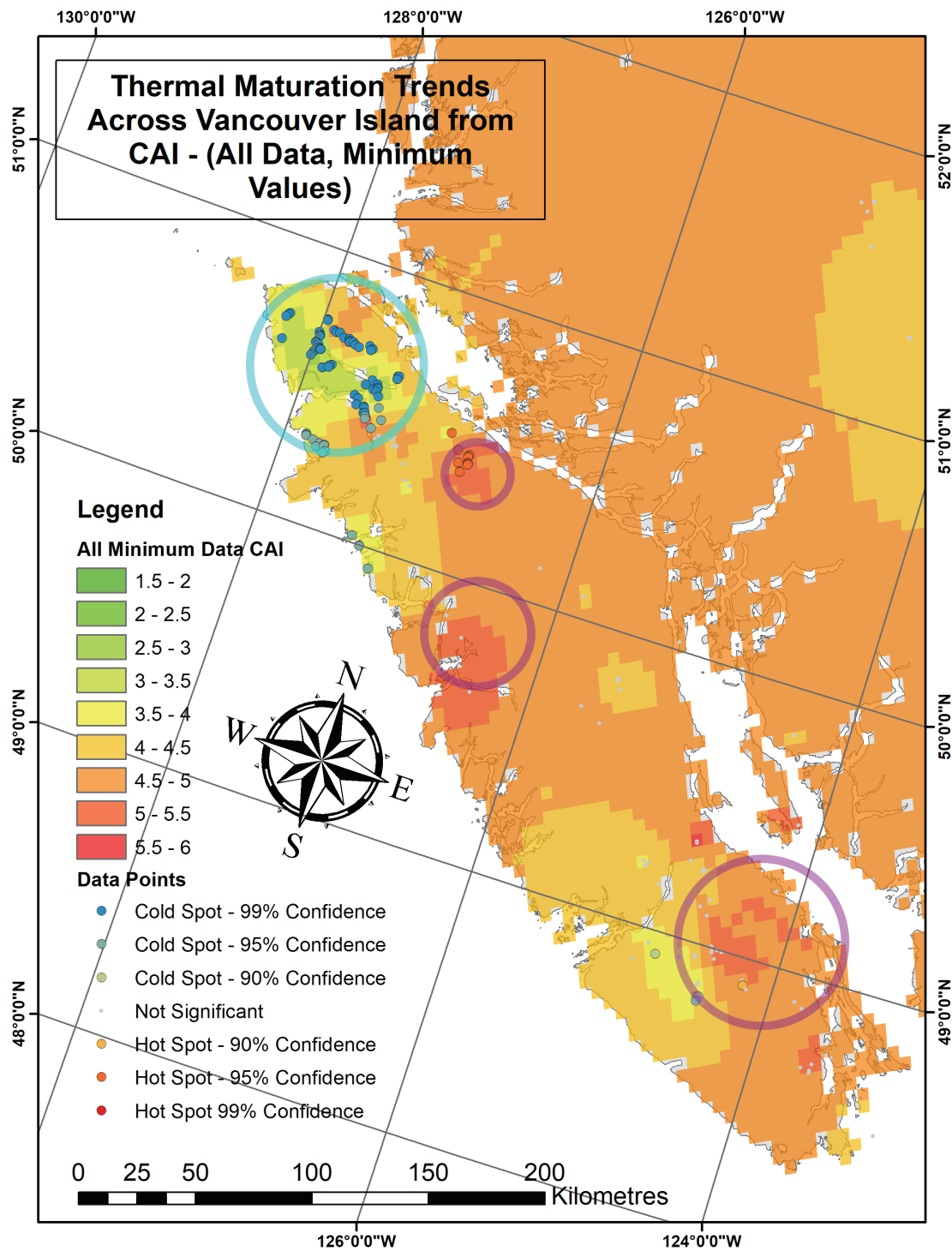


Figure 11: Thermal maturation trends across Vancouver Island from CAI. All data included; minimum values. Hotspots are circled in purple, while cold spots are circled in blue.

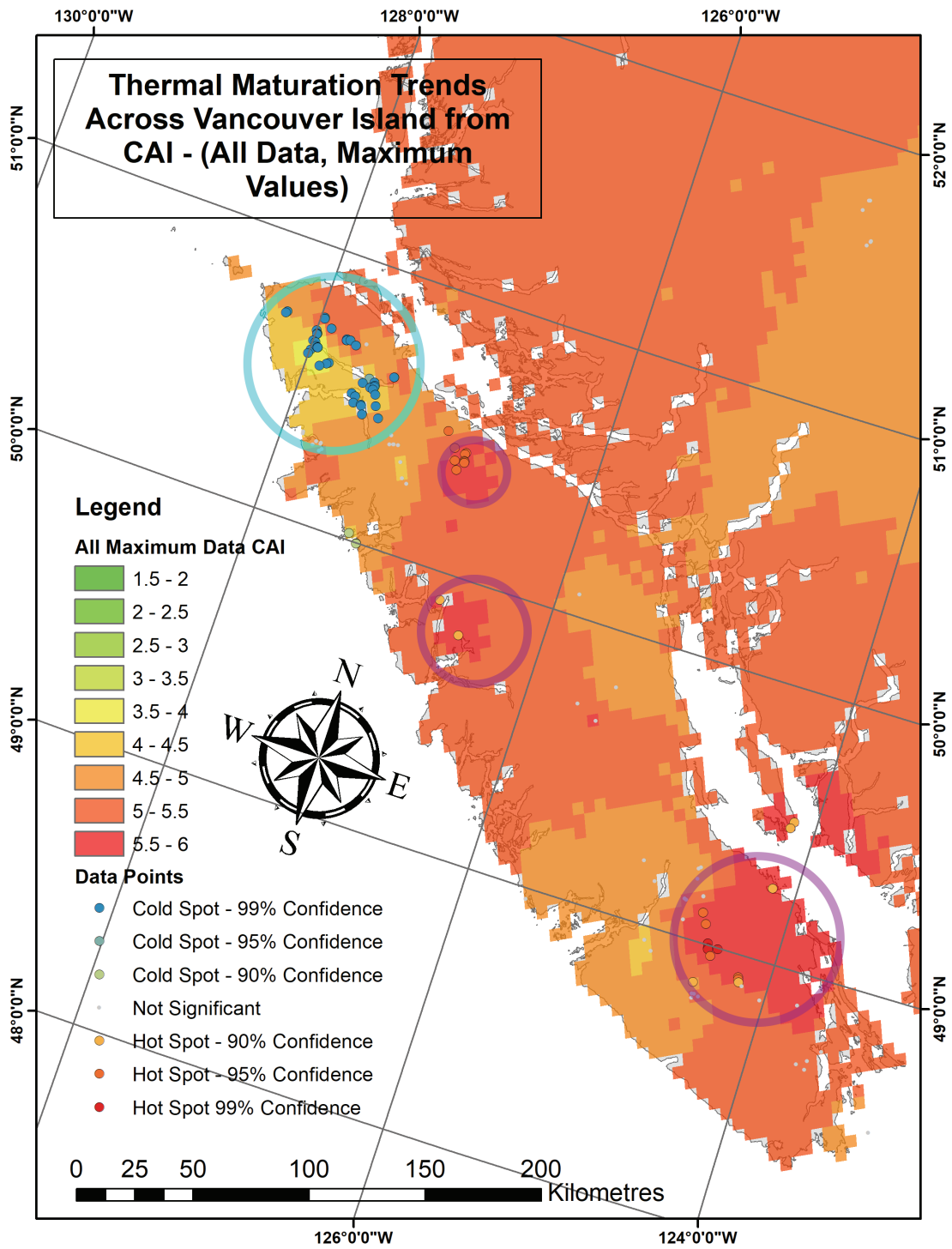


Figure 12: Thermal maturation trends across Vancouver Island from CAI. All data included; maximum values. Hotspots are circled in purple, while cold spots are circled in blue.

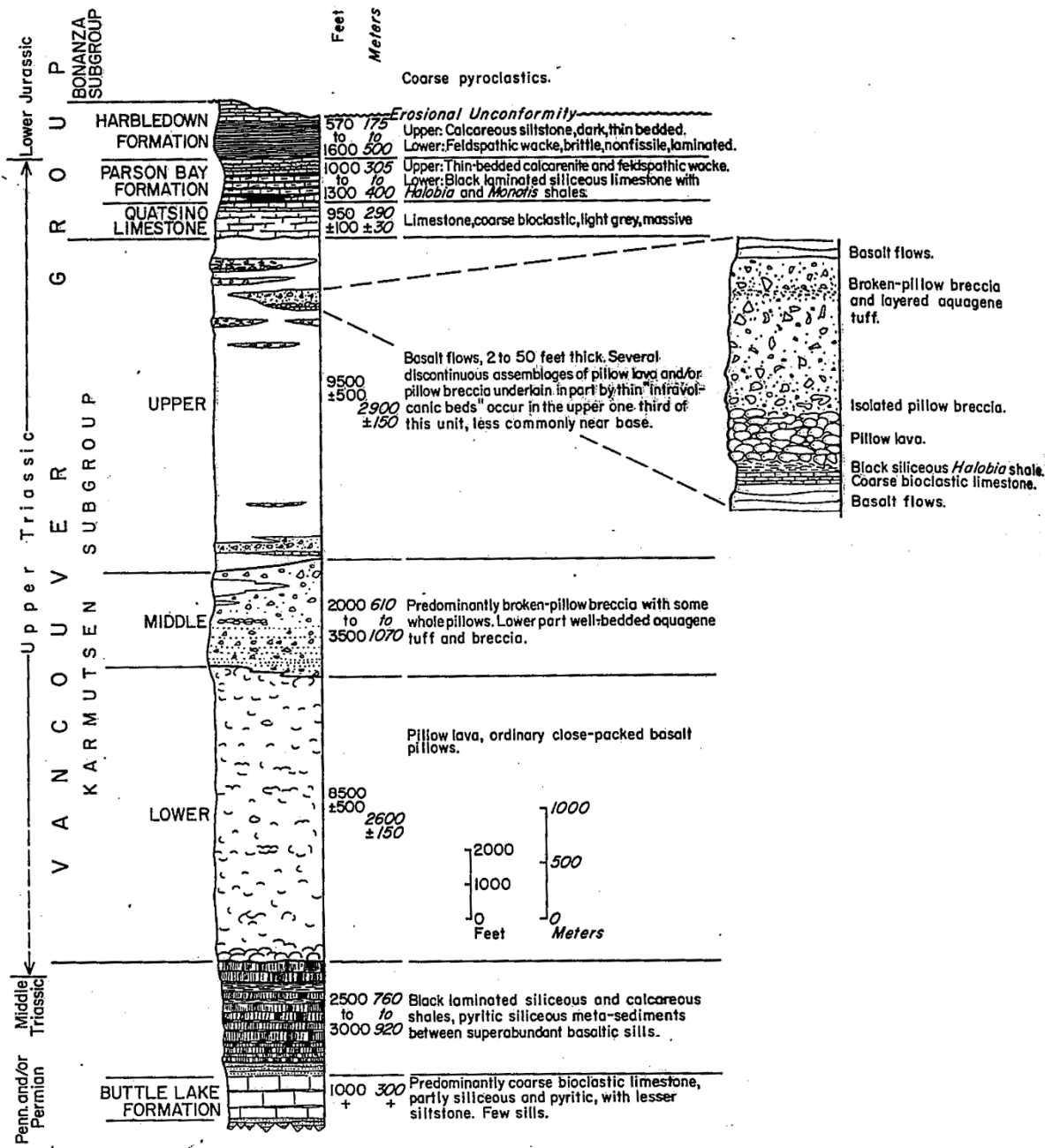


Figure 13: Stratigraphy of northeastern Vancouver Island. From Carlisle and Suzuki (1974).

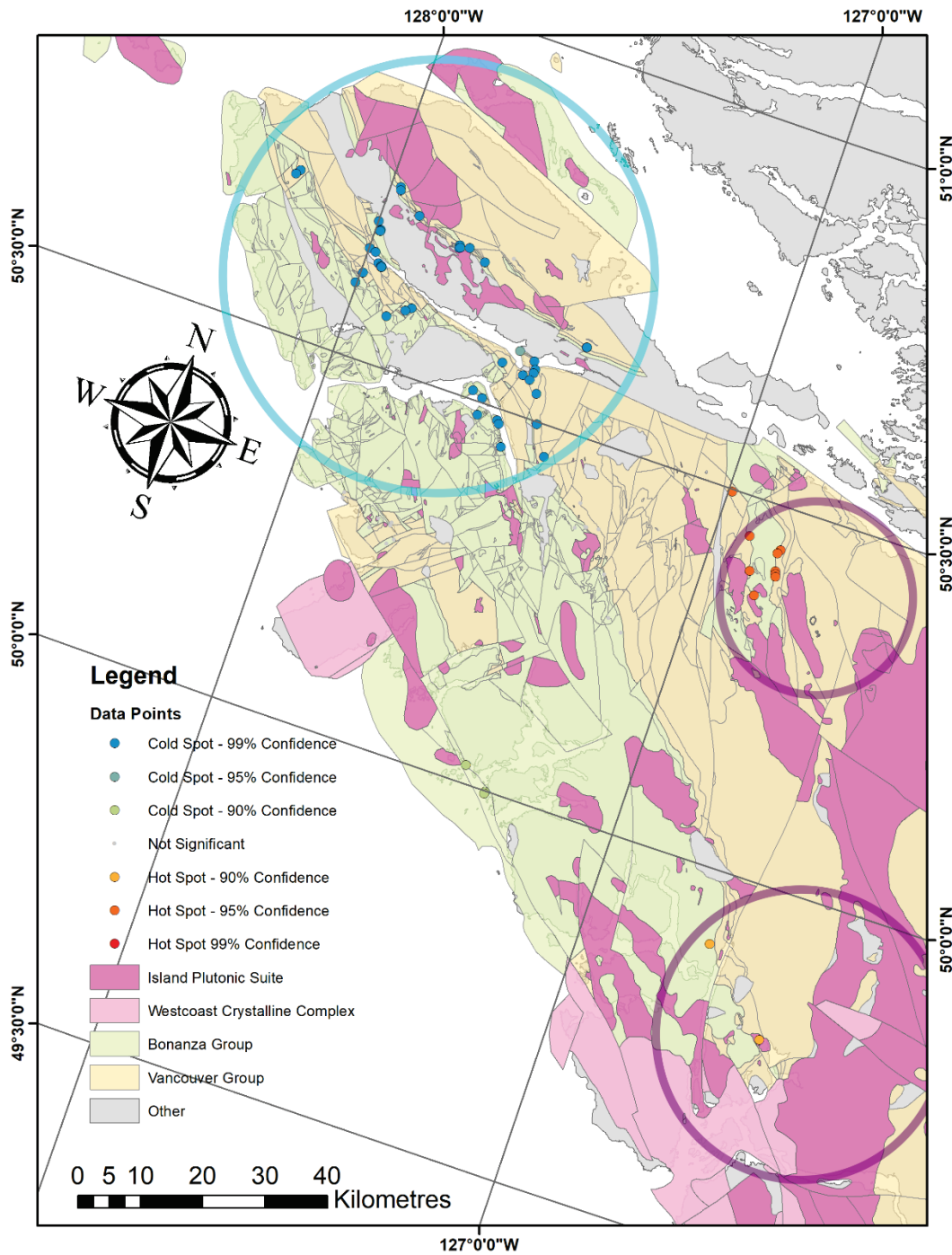


Figure 14: Lithological associations proximal to the central and northern Vancouver Island thermal hot spots, as well as to the thermal cold spot on the northern tip of the island. Hotspots are circled in purple, while the cold spot is circled in blue. Lithology map from the British Columbia Geological Survey (2018).

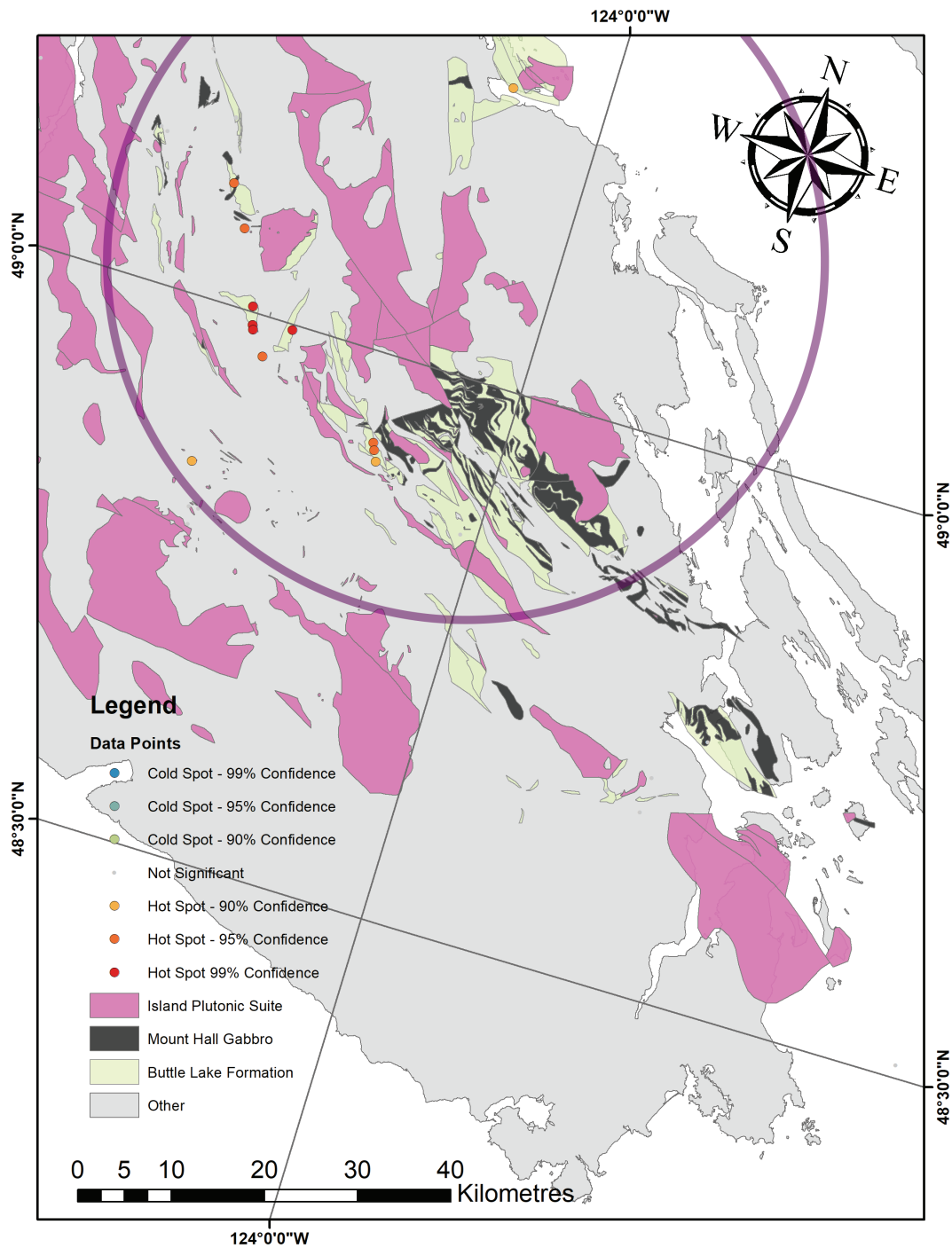


Figure 15: Lithological associations proximal to the southern Vancouver Island thermal hot spot. The hotspot is circled in purple. Lithology map from the British Columbia Geological Survey, (2018).

Challenges in Assembling Cordilleran $\delta^{13}\text{C}$ Records

The background CAI values of approximately 4 to 5 across the Canadian Cordillera are problematic for studies that utilize $\delta^{13}\text{C}$ to interpret paleoenvironmental conditions (Figure 5; Figure 6). This is because the primary $\delta^{13}\text{C}$ signal can be compromised by fluid-rock interactions, an effect that has even been observed in carbonates that experienced lower maximum burial temperatures than that represented by a CAI of 4 (e.g. Banner and Hanson, 1990; Derry, 2010). A loss of primary signal via this process can result in a strong correlation between $\delta^{13}\text{C}$ and $\delta^{18}\text{O}$ (Marshall, 1992).

To either side of the British Columbia and Yukon border, the Sinwa and Aksala Formations are comprised of possibly coeval Late Triassic limestone (Lowey et al., 2009). Two stratigraphic sections investigated in British Columbia of the Sinwa Formation both preserved primary $\delta^{13}\text{C}$ signals, whereas another two stratigraphic sections investigated in Yukon of the Aksala Formation both showed strong correlation between $\delta^{13}\text{C}$ and $\delta^{18}\text{O}$ (Lei et al., 2019). Although both Sinwa and Aksala formation localities are within thermal alteration cold spots, localities within the Sinwa Formation fall much closer to the center of its respective cold spot (Figure 16; Figure 17). Localities in the Aksala Formation are on the very edge of its cold spot, and also quite close to a large hot spot directly to the east (Figure 16; Figure 17).

Near the northern tip of Vancouver Island, two stratigraphic sections were investigated through the Late Triassic limestone of the Quatsino and Parsons Bay Formations (Muller, 1977; Massey and Friday, 1987). These were the northern Holberg section which preserved primary $\delta^{13}\text{C}$ signal, and the more southern Yreka section which did not (Vanwieren, 2019). Similarly to the Sinwa and Aksala Formation localities, both Holberg and Yreka are within thermal alteration cold spots, but the Yreka locality with a compromised $\delta^{13}\text{C}$ record falls very near the edge of the cold spot, and away from the minimum CAI center (Figure 18; Figure 19).

This preliminary analysis suggests there may be a significant correlation between the location of a section relative to thermal alteration cold spots and the preservation of a primary $\delta^{13}\text{C}$ signal at that section. Future studies involving $\delta^{13}\text{C}$ in the Canadian Cordillera might increase their success rate by considering CAI cold spots as a factor in the locality selection process.

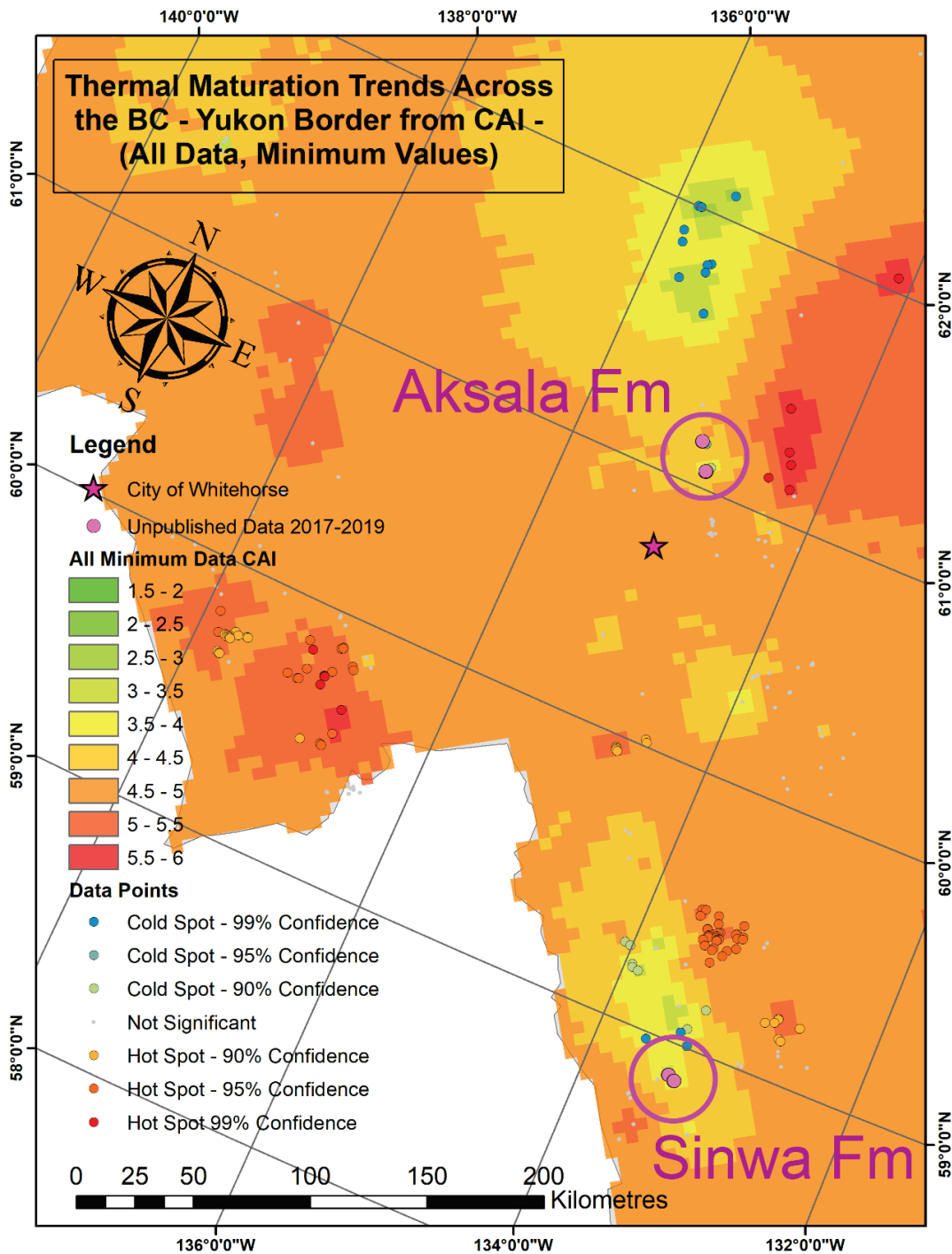


Figure 16: Thermal maturation trends across the western British Columbia - Yukon border region from CAI. All data included; minimum values. The Sinwa Formation samples, which preserve primary $\delta^{13}\text{C}$ signals, falls much closer to the center of its cold spot than the Aksala Formation samples which do not preserve primary $\delta^{13}\text{C}$ signals.

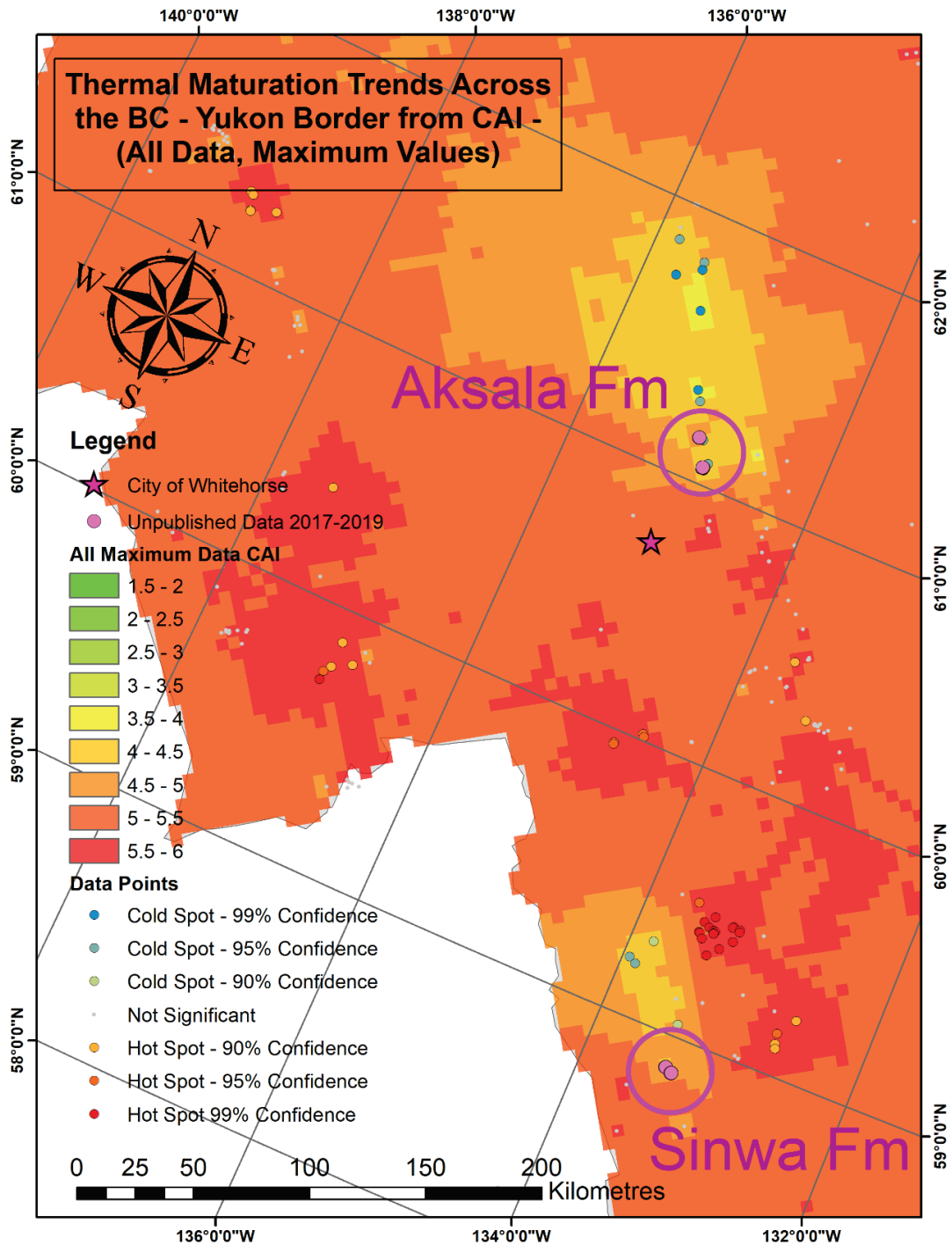


Figure 17: Thermal maturation trends across the western British Columbia - Yukon border region from CAI. All data included; maximum values. The Sinwa Formation samples, which preserve primary $\delta^{13}\text{C}$ signals, falls much closer to the center of its cold spot than the Aksala Formation samples which do not preserve primary $\delta^{13}\text{C}$ signals.

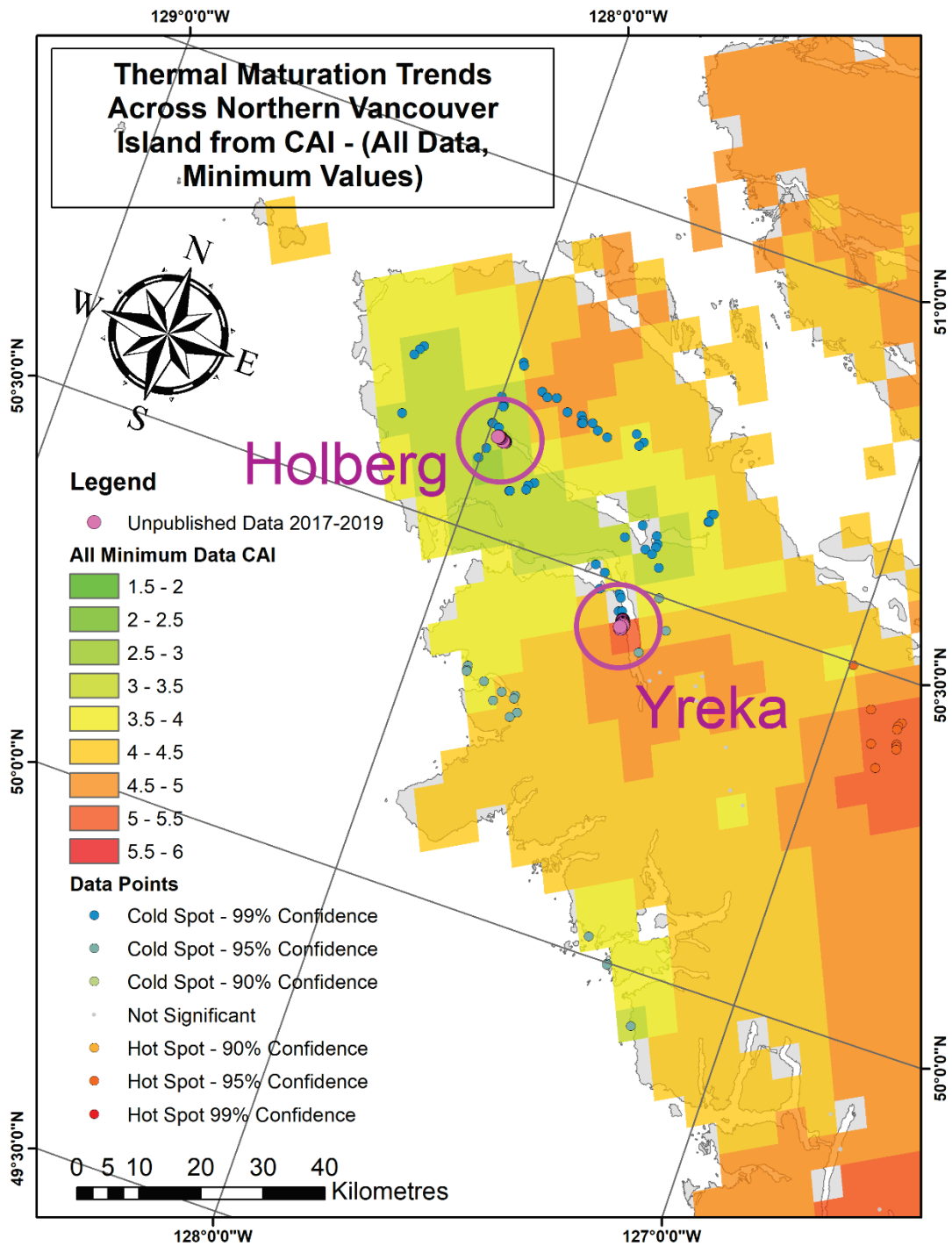


Figure 18: Thermal maturation trends across the northern tip of Vancouver Island from CAI. All data included; minimum values. The Holberg section samples, which preserve primary $\delta^{13}\text{C}$ signals, falls much closer to the center of its cold spot than the Yreka section samples which do not preserve primary $\delta^{13}\text{C}$ signals.

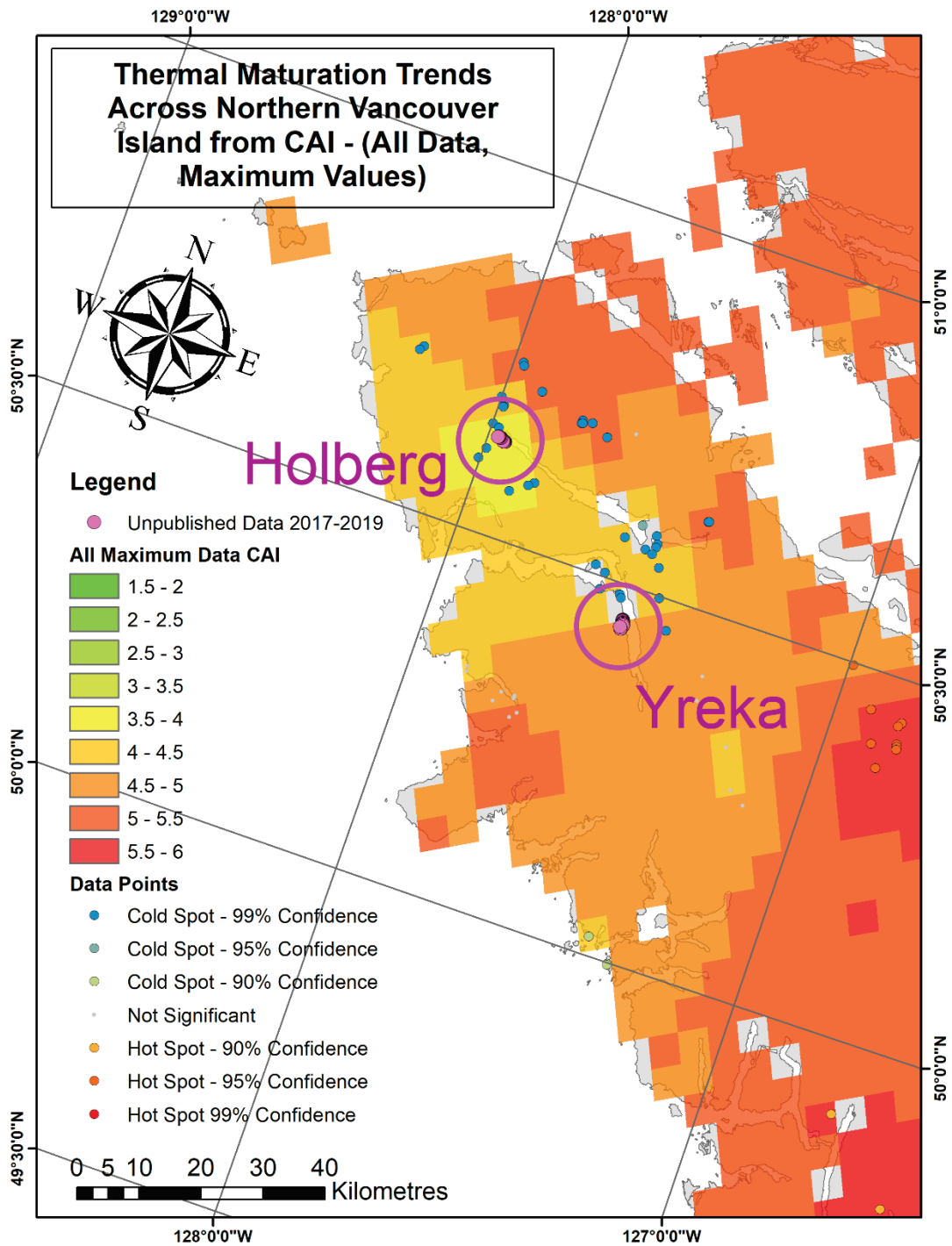


Figure 19: Thermal maturation trends across the northern tip of Vancouver Island from CAI. All data included; maximum values. The Holberg section samples, which preserve primary $\delta^{13}\text{C}$ signals, falls much closer to the center of its cold spot than the Yreka section samples which do not preserve primary $\delta^{13}\text{C}$ signals.

Limitations

Many limitations of this technique arise from the distribution of the conodont collections data. Inherent to outcrop sampling, the CAI values and trends can only represent conodont-bearing lithologies exposed at the surface, and therefore assumes continuous distribution of such lithologies by interpolation. Lithologies such as igneous, metamorphic, and non-marine sedimentary units are not represented, nor are any subsurface units. Since the extinction of conodonts occurred at the Triassic - Jurassic boundary (e.g. Clark, 1983), any younger units are also not represented. These limitations should be taken into consideration when utilizing the hot spot map for interpreting general thermal alteration trends. Large stretches of the Canadian Cordillera have very sparse conodont collection datapoints, such as west-central BC, and the far north of Yukon, resulting in very uncertain interpolated values and trends for these regions (Figure 5; Figure 6). The GPS coordinates for older collections are likely imprecise by modern standards, but trial interpolations excluding historical collections confirm this is not problematic given the regional scale of this study. Therefore, older collections are included. Collections are highly clustered by study locality, and this was addressed by using the Kriging method.

Additional limitations are associated with uncertainties in CAI geothermometry. As a semi-quantitative method, assignment of a CAI value to a specimen depends on an individual researcher's qualitative judgement of colour. For specimens that undergo brief but intense heating, such is the case for contact metamorphism, there can be CAI variation within a small area and even within a single specimen (Wiederer et al., 2002). Specimens can also lose organic material from metasomatic processes, including interaction with meteoric, saline, and hydrothermal fluids (Wiederer et al., 2002). These processes do not follow the thermal progression of the CAI, and therefore cannot be interpreted with the same corresponding temperature ranges (Wiederer et al., 2002). Research into using Iterative Fitting of Raman Spectra (IFORS) to determine maximum temperature of conodont specimens independently of CAI has found the range of temperatures associated with each CAI value may be significantly different than previously established (McMillan and Golding, 2019). The influence on CAI from diagenetic processes besides thermal alteration, as well as complex thermal histories, have been indicated as likely sources of discrepancy between maximum temperature values obtained via CAI and IFORS (McMillan and Golding, 2019).

CONCLUSIONS

Spatial analysis of CAI with GIS is a tool that has not been previously used on a regional scale in Western Canada, which is an ideal investigative target given the existence of extensive conodont collections from this area. This study creates a thermal maturation hot spot map of the Canadian Cordillera based on CAI, and has the potential to assist in a multitude of fields, from Cordilleran tectonic reconstruction to preliminary assessment in hydrocarbon exploration. Major hot spots include the southeast corner of British Columbia, the central coast of British Columbia, southern Vancouver Island, and most of the British Columbia - Yukon border. Major cold spots include the northeast quadrant of British Columbia, the northern tip of Vancouver Island, and central Haida Gwaii. Important limitations of this analysis include the fact that interpolated values are only representative of conodont-bearing lithologies exposed at surface, and that widely varying sample density between regions will affect the quality of analysis depending on the locality of study.

Statistically significant hot spots on Vancouver Island are found to align with the prevalence of intrusive units. The most prominent hot spot is located in the southern portion of the island, where extensive exposures of Permian limestone are uniquely found. This unit is more thermally altered than the Triassic limestone prevalent farther north on the island.

When evaluating paleoenvironmental studies that utilize the $\delta^{13}\text{C}$ isotope record near the BC - Yukon border, and from the northern end of Vancouver Island, those that preserve primary $\delta^{13}\text{C}$ signals were close to the centre of thermal alteration cold spots. Future sites for proxy record measurements should consider regional spatial patterns in thermal alteration to increase the likelihood of success.

ACKNOWLEDGEMENTS

This study was initially conducted as a term project for a graduate course GEOG 520 - Introductory GIS for Graduate Research, at the University of Victoria. The authors would like to thank Hillary Taylor (Geological Survey of Canada - Pacific) for assistance with obtaining the conodont collections data; Jessica Fitterer (University of Victoria) for guidance with ArcGIS and assisting with specific geospatial techniques; Rebecca Morris (University of Victoria) for sharing her knowledge of Vancouver Island geology and the cooking of its carbonates in particular; Rob MacNaughton (Geological Survey of Canada - Calgary) for providing a thorough review of the manuscript; and Nathan Cleven (Geological Survey of Canada - Pacific) for checking the GIS shapefiles.

REFERENCES

Banner, J. L., and Hanson, G. N. (1990). Calculation of simultaneous isotopic and trace-element variations during water-rock interaction with applications to carbonate diagenesis. *Geochimica et Cosmochimica Acta*; v. 54; p. 3123-3137.

British Columbia Geological Survey. (2018). MapPlace GIS internet mapping system; British Columbia Ministry of Energy, Mines and Petroleum Resources; Retrieved from <http://www.MapPlace.ca>.

Belasky, P., Stevens, C.H., and Hanger, R.A. (2002). Early Permian location of western North American terranes based on brachiopod, fusulinid, and coral biogeography. *Palaeogeography, Palaeoclimatology, Palaeoecology*; v. 179; p. 245-266.

Beranek, L.P., and Mortensen, J.K. (2011). The timing and provenance record of the Late Permian Klondike orogeny in northwestern Canada and arc-continent collision along western North America. *Tectonics*; v. 30; p. 1-23.

Carlisle, D., and Suzuki, T. (1974). Emergent basalt and submergent carbonate-clastic sequences including the Upper Triassic Dilleri and Welleri zones on Vancouver Island. *Canadian Journal of Earth Sciences*; v. 11; p. 254-279.

Clark, D. L. (1983). Extinction of Conodonts. *Journal of Paleontology*; v. 57; n. 4; p. 652-661.

Colpron, M., and Nelson, J. L. (2011). A digital atlas of terranes for the northern Cordillera. BC GeoFile; 11.

Colpron, M., Nelson, J. L., and Murphy, D. C. (2007). Northern Cordilleran terranes and their interactions through time. *GSA today*; v. 17; n. 4/5; p. 4-10.

DeBari, S. M., Anderson, R. G., and Mortensen, J. K. (1999). Correlation among lower to upper crustal components in an island arc: the Jurassic Bonanza arc, Vancouver Island, Canada. *Canadian Journal of Earth Sciences*; v. 36; p. 1371-1413.

Derry, L. A. (2010). A burial diagenesis origin for the Ediacaran Shuram-Wonoka carbon isotope anomaly. *Earth and Planetary Science Letters*; v. 294; p. 152-162.

D'Souza, R. J., Canil, D., and Creaser, R. A. (2015). Assimilation, differentiation, and thickening during formation of arc crust in space and time: The Jurassic Bonanza arc, Vancouver Island, Canada. *Geological Society of America Bulletin*; v. 128 (3-4); p. 543-557.

Epstein, A. G., Epstein, J. B., and Harris L. D. (1977). Conodont color alteration: and index to organic metamorphism. *United States Geological Survey Professional Paper*; n. 995; p. 1-27.

esri. (n.d.). ArcGIS for Desktop. Retrieved November 12, 2019, from <https://desktop.arcgis.com/en/arcmap/10.3/tools/spatial-statistics-toolbox/hot-spot-analysis.htm>.

Gawlick, H. J., Krystyn, L., and Lein, R. (1994). Conodont colour alteration indices: Palaeotemperatures and metamorphism in the Northern Calcareous Alps—a general view. *Geologische Rundschau*; v. 83(3); p. 660-664.

Harris, A. G., Wardlaw, B. R., Rust, C. C., and Merrill, G. K. (1980). Maps for assessing thermal maturity (conodont color alteration index maps) in Ordovician through Triassic rocks in Nevada and Utah and adjacent parts of Idaho and California (n. 1249).

Johnston, S. T. (2008). The Cordilleran Ribbon Continent of North America. *Annual Review of Earth and Planetary Sciences*; v. 36; p. 495-530.

Jones, D. L., Silberling, N. J., and Hillhouse, J. (1977). Wrangellia – A displaced terrane in northwestern North America. *Canadian Journal of Earth Sciences*; v. 14; p. 2565-2577.

Kent, D.V., and Irving, E. (2010). Influence of inclination error in sedimentary rocks on the Triassic and Jurassic apparent pole wander path for North America and implications for Cordilleran tectonics. *Journal of Geophysical Research*; v. 115; p. 1-25.

Königshof, P. (2003). Conodont deformation patterns and textural alteration in Paleozoic conodonts: examples from Germany and France. *Senckenbergiana lethaea*; v. 83(1-2); p. 149-156.

Legall, F. D., Barnes, C. R., and Macqueen, R. W. (1981). Thermal Maturation, Burial History and Hotspot Development, Paleozoic Strata of Southern Ontario – Quebec, from Conodont and Acritarch Colour Alteration Studies. *Bulletin of Canadian Petroleum Geology*; v. 29; n. 4; p. 492-539.

Lei, J. Z. X., Golding, M. L., and Husson, J. M. (2019). Paleoenvironmental Interpretation and Identification of the Norian – Rhaetian Boundary in the Whitehorse Trough (Stikine Terrane, Northern Canadian Cordillera). *Geological Association of America Annual Meeting 2019*; Phoenix Arizona, September 22-25. *Abstracts with Programs*; v. 51; n. 5; 117(5).

Lowey, G.W., Long, D.G.F., Fowler, M.G., Sweet, A.R., and Orchard, M.J. (2009). Petroleum source rock potential of Whitehorse trough: a frontier basin in south-central Yukon. *Bulletin of Canadian Petroleum Geology*; v. 57; n. 3; p. 350-386.

MacNaughton, R.B., Fallas, K.M., and Zantvoort, W. (2008). Qualitative assessment of the Plateau Fault (Mackenzie Mountains, NWT) as a conceptual hydrocarbon play. *Geological Survey of Canada Open File 5831*; 33 p.

McMillan, R., and Golding, M. (2019). Thermal maturity of carbonaceous material in conodonts and the Color Alteration Index: Independently identifying maximum temperature with Raman spectroscopy. *Palaeogeography, Palaeoclimatology, Palaeoecology*; v. 534; n. 109290.

Marshall, J. D. (1992). Climatic and oceanographic isotopic signals from the carbonate rock record and their preservation. *Geological Magazine*; v. 129; p. 143-160.

Massey, N. W. D., and Friday, S. J. (1987). *Geology of the Cowichan Lake Area, Vancouver Island*. British Columbia Ministry of Energy, Mines and Petroleum Resources; *Geological Fieldwork*; 1987-1; p. 223-229.

- Mihalynuk, M.G., Nelson, J.A., and Diakow, L.J., 1994. Cache Creek terrane entrapment: oroclinal paradox within the Canadian Cordillera. *Tectonics*; v. 13; p. 575–595.
- Monger, J. W. H. (1977). Upper Paleozoic rocks of the western Canadian Cordillera and their bearing on Cordilleran evolution. *Canadian Journal of Earth Sciences*; v. 14; p. 1832-1859.
- Monger, J. W. H. (1997). Plate tectonics and northern Cordilleran geology: an unfinished revolution. *Geoscience Canada*; v. 24; n. 4; p. 189-198.
- Monger, J. W. H., and Ross, C. A. (1971). Distribution of Fusulinaceans in the Western Canadian Cordillera. *Canadian Journal of Earth Sciences*; v. 8; p. 259-278.
- Muller, J. E. (1977). *Geology of Vancouver Island*. Geological Association of Canada; Joint Annual Meeting 1977; Field Trip 7 Guidebook.
- Nelson, J. L., and Colpron, M. (2007). Tectonics and metallogeny of the British Columbia, Yukon and Alaskan Cordillera, 1.8 Ga to the present. *Mineral Deposits of Canada: A Synthesis of Major Deposit-Types, District Metallogeny, the Evolution of Geological Provinces, and Exploration Methods*. Edited by WD Goodfellow. Geological Association of Canada, Mineral Deposits Division, Special Publication; v. 5; p. 755-791.
- Orchard, M.J. and Forster, P.J.L. (1991). Conodont colour and thermal maturity of the Late Triassic Kunga Group, Queen Charlotte Islands, British Columbia. *Evolution and Hydrocarbon Potential of the Queen Charlotte Basin, British Columbia*, Geological Survey of Canada, Paper 90 - 10; p. 453-464
- Read, P. B., Psutka, J. F., and Phillipone, J. (1991a). Organic Maturity Data for the Canadian Cordillera. Geological Survey of Canada; Open File; n. 2341.
- Read, P. B., Woodsworth, G. J., Greenwood, H. J., Ghent, E. D., and Evenchick, C. A. (1991b). Metamorphic map of the Canadian Cordillera / Carte métamorphique de la Cordillère Canadienne. Geological Survey of Canada; A Series Map; 1714A; scale 1:2 000 000.
- Rejebian, V. A., Harris, A. G., and Huebner, J. S. (1987). Conodont Color and Textural Alteration: An Index to Regional Metamorphism, Contact Metamorphism, and Hydrothermal Alteration. *Geological Society of America Bulletin*; v. 99; p. 471-479.

Scheeres, A. (2016). Kriging: Spatial Interpolation in Desktop GIS. Azavea. Retrieved November 12, 2019, from <https://www.azavea.com/blog/2016/09/12/kriging-spatial-interpolation-desktop-gis/>.

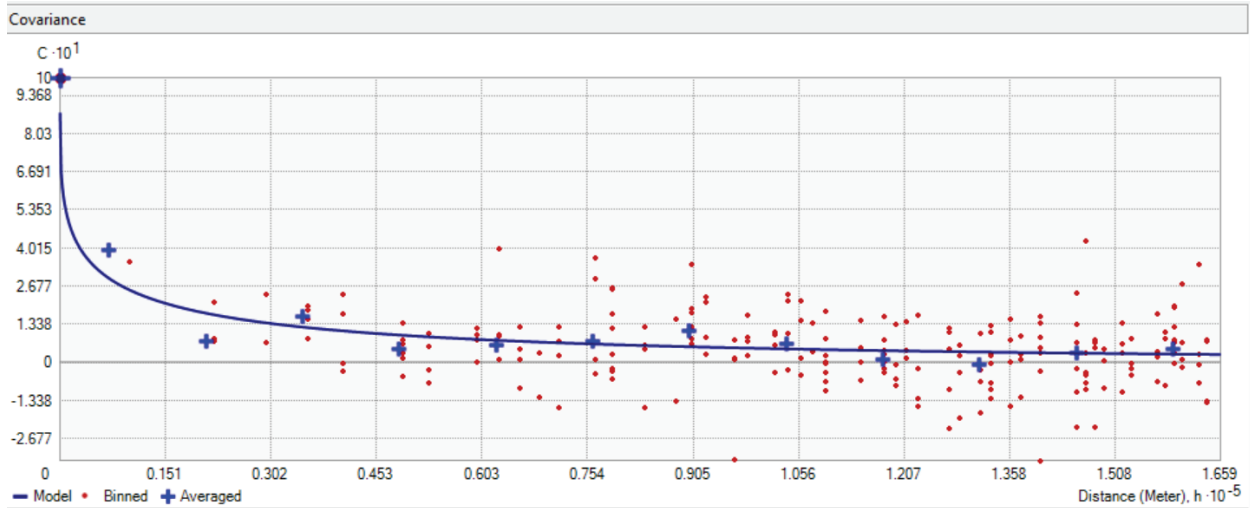
Vanwieren, C. S. (2019). Characterizing the Triassic - Jurassic Boundary Through Stratigraphy of Northern Vancouver Island Carbonates. Unpublished Honours Thesis; University of Victoria; Victoria, British Columbia.

Wardlaw, B. R., and Harris, A. G. (1984). Conodont-based thermal maturation of Paleozoic rocks in Arizona. AAPG Bulletin; v. 68; n. 9; p. 1101-1106.

Wiederer, U., Königshof, P., Feist, R., Franke, W., and Doublier, M. P. (2002). Low-grade metamorphism in the Montagne Noire (S-France): Conodont Alteration Index (CAI) in Palaeozoic carbonates and implications for the exhumation of a hot metamorphic core complex. Schweizerische Mineralogische und Petrographische Mitteilungen; v. 82; p. 393-407.

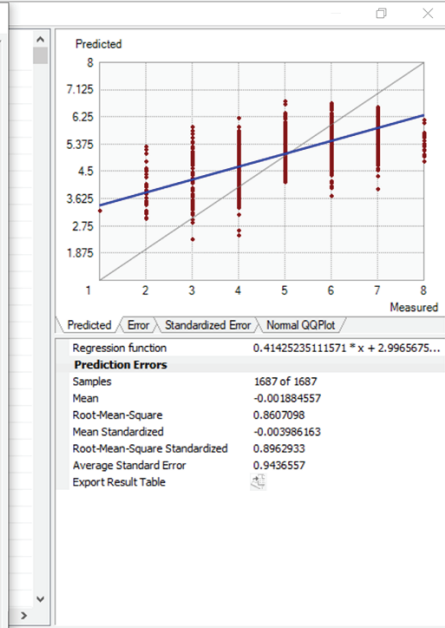
APPENDIX – KRIGING PROCESS AND MODEL FITTING

All Data, Max CAI

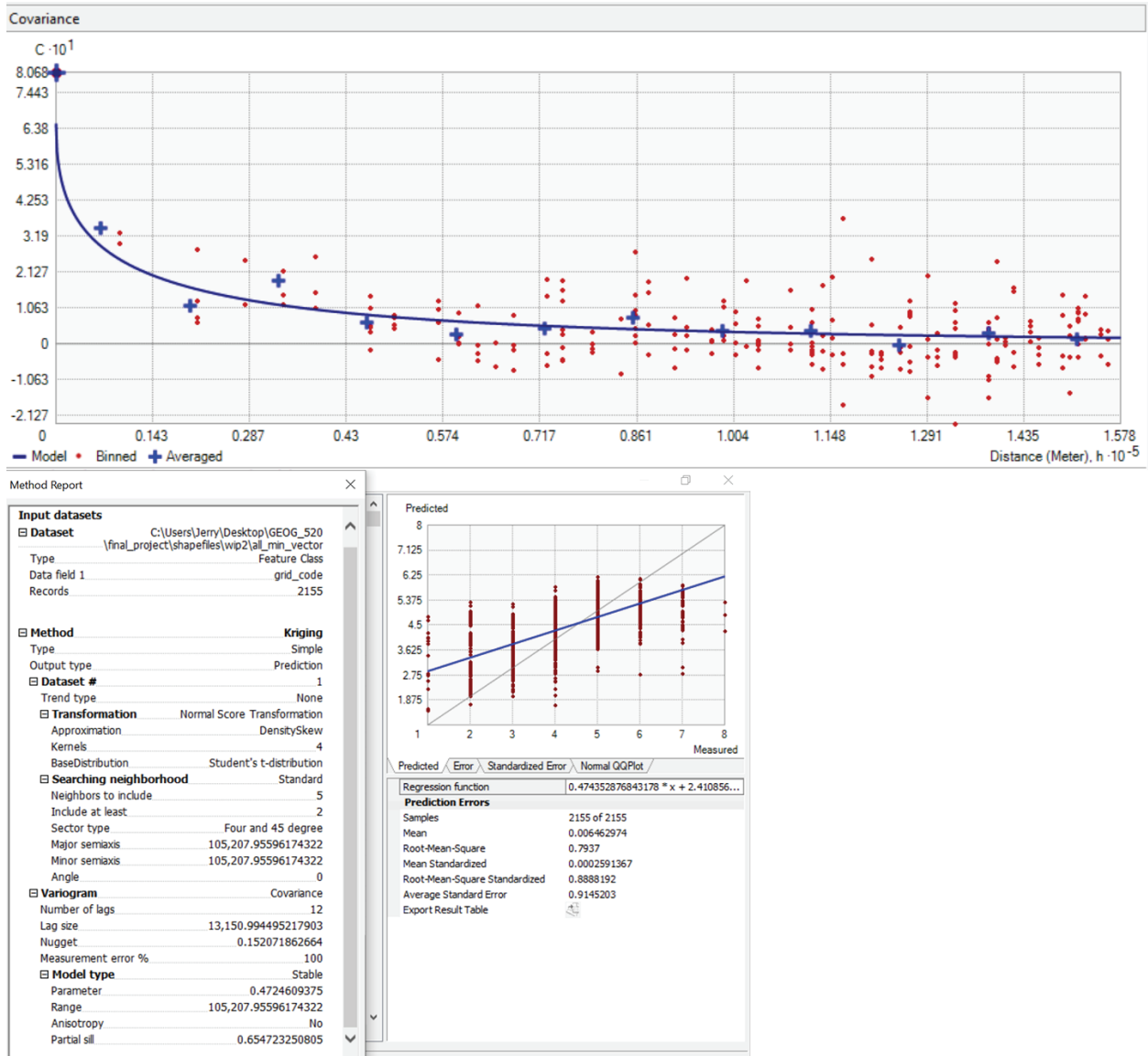


Method Report

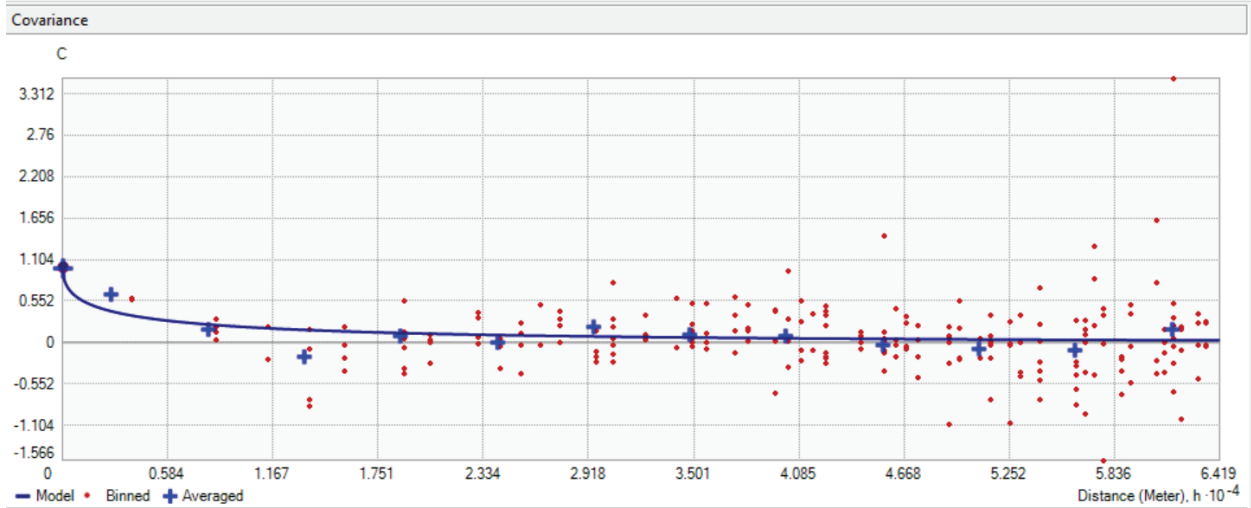
Dataset	
Type	Feature Class
Data field 1	grid_code
Records	1687
Method	
Type	Kriging
Output type	Prediction
Dataset #	
Trend type	None
Transformation	
Approximation	DensitySkew
Kernels	1
BaseDistribution	Empirical
Searching neighborhood	
Neighbors to include	5
Include at least	2
Sector type	Four and 45 degree
Major semiaxis	110,614.9434148061
Minor semiaxis	110,614.9434148061
Angle	0
Variogram	
Number of lags	12
Lag size	13,826.867926850762
Nugget	0.123339305863
Measurement error %	100
Model type	
Parameter	0.3669921875
Range	110,614.9434148061
Anisotropy	No
Partial sill	0.876654529651



All Data, Min CAI



Wrangell Terrane Only, Max CAI



Method Report

Input datasets

- Dataset: C:\Users\Jerry\Desktop\GEOG_520\final_project\shapefiles\wp2\all_max_wrangell
- Type: Feature Class
- Data field 1: grid_code
- Records: 202

Method **Kriging**

- Type: Simple
- Output type: Prediction

Dataset # 1

- Trend type: None

Transformation Normal Score Transformation

- Approximation: DensitySkew
- Kernels: 1
- BaseDistribution: Empirical

Searching neighborhood Standard

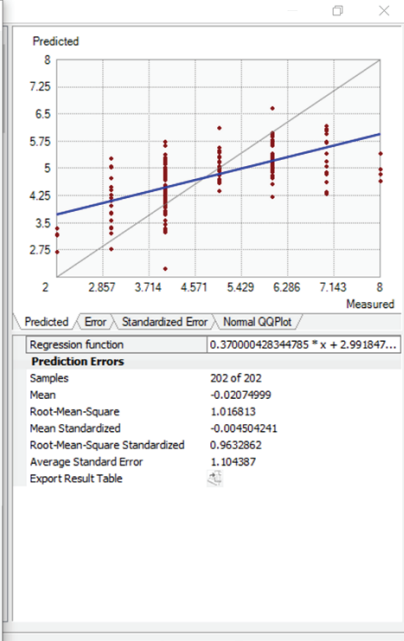
- Neighbors to include: 5
- Include at least: 2
- Sector type: Four and 45 degree
- Major semiaxis: 42,794.415888605385
- Minor semiaxis: 42,794.415888605385
- Angle: 0

Variogram Covariance

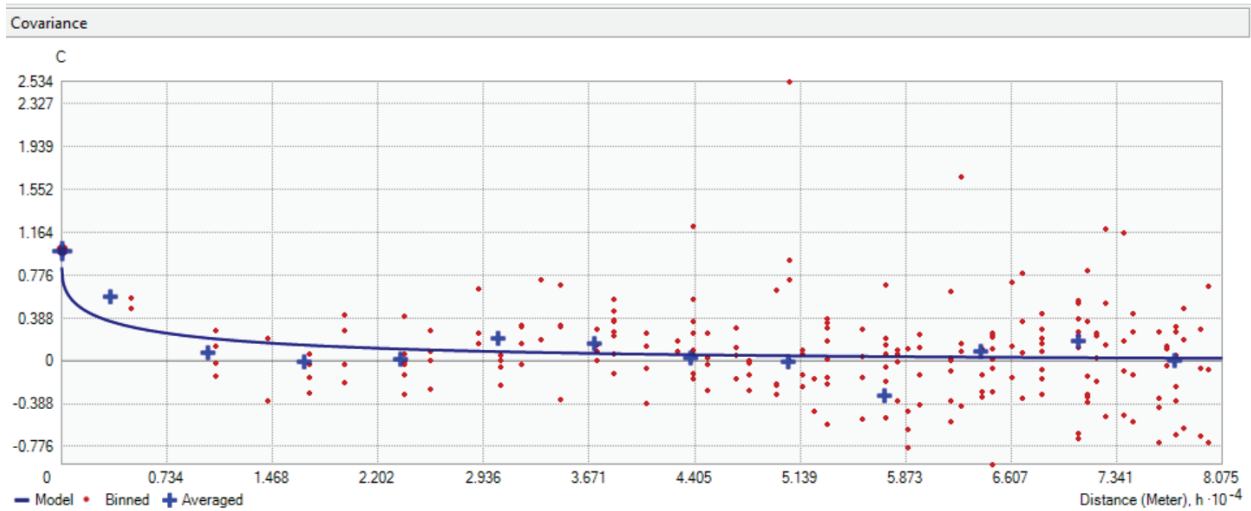
- Number of lags: 12
- Lag size: 5,349.301986075673
- Nugget: 0
- Measurement error %: 100

Model type Stable

- Parameter: 0.43203125
- Range: 42,794.415888605385
- Anisotropy: No
- Partial sill: 1.035124687713



Wrangell Terrane Only, Min CAI



Method Report

Input datasets

Dataset: C:\Users\Jerry\Desktop\GEOG_520
 \final_project\shapefiles\wp2\al_min_wrangel

Type: Feature Class
 Data field 1: grid_code
 Records: 221

Method: Kriging
 Type: Simple
 Output type: Prediction

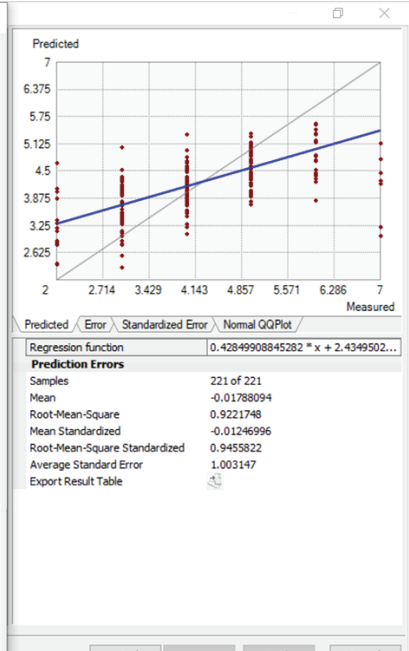
Dataset #: 1
 Trend type: None

Transformation: Normal Score Transformation
 Approximation: DensitySkew
 Kernels: 1
 BaseDistribution: Log-empirical

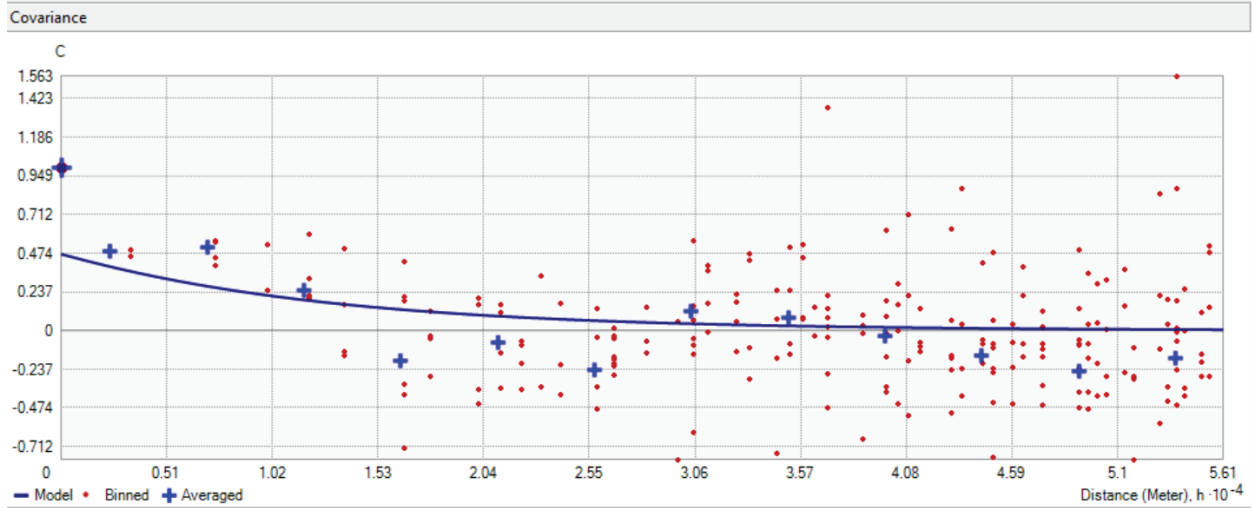
Searching neighborhood: Standard
 Neighbors to include: 5
 Include at least: 2
 Sector type: Four and 45 degree
 Major semiaxis: 53,834.15885765152
 Minor semiaxis: 53,834.15885765152
 Angle: 0

Variogram: Covariance
 Number of lags: 12
 Lag size: 6,729.26985720644
 Nugget: 0.152016400328
 Measurement error %: 100

Model type: Stable
 Parameter: 0.4513671875
 Range: 53,834.15885765152
 Anisotropy: No
 Partial sill: 0.847988227101



Stikine Terrane Only, Max CAI



Method Report

Input datasets

- Dataset: C:\Users\Jerry\Desktop\GEOG_520\final_project\shapefiles\wp2\stl_max_stikine
- Type: Feature Class
- Data field 1: grid_code
- Records: 292

Method

- Method: Kriging
- Type: Simple
- Output type: Prediction

Dataset #

- Dataset #: 1
- Trend type: None

Transformation

- Transformation: Normal Score Transformation
- Approximation: DensitySkew
- Kernels: 1
- BaseDistribution: Log-empirical

Searching neighborhood

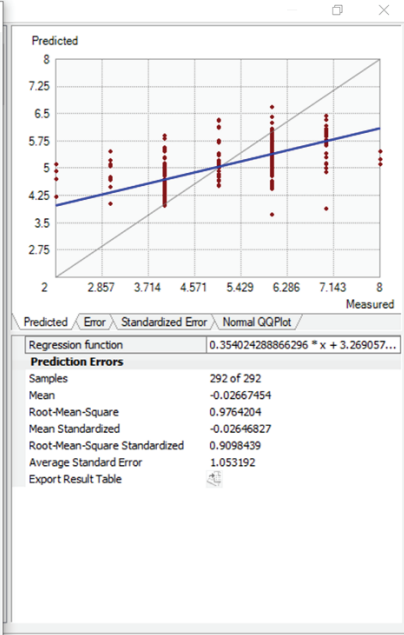
- Searching neighborhood: Standard
- Neighbors to include: 5
- Include at least: 2
- Sector type: Four and 45 degree
- Major semiaxis: 37,402.99336392656
- Minor semiaxis: 37,402.99336392656
- Angle: 0

Variogram

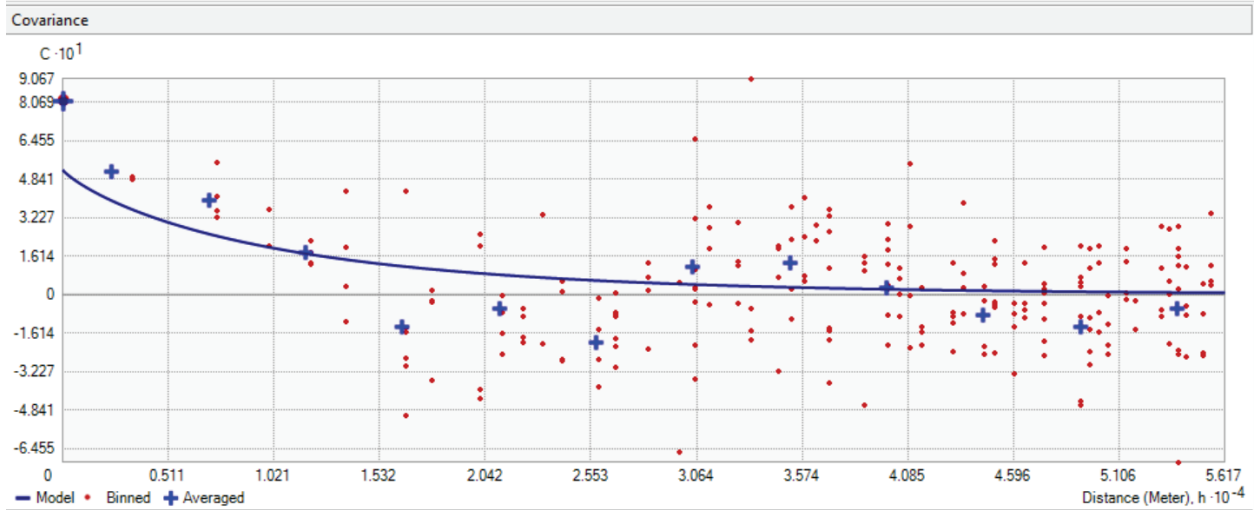
- Variogram: Covariance
- Number of lags: 12
- Lag size: 4,675.37417049082
- Nugget: 0.531521013136
- Measurement error %: 100

Model type

- Model type: Stable
- Parameter: 1.02265625
- Range: 37,402.99336392656
- Anisotropy: No
- Partial sill: 0.468421347665



Stikine Terrane Only, Min CAI



Method Report

Input cases

- Dataset: C:\Users\Jerry\Desktop\GEOG_520\final_project\shapefiles\wp2\all_min_stikine
- Type: Feature Class
- Data field 1: grid_code
- Records: 452

Method **Kriging**

- Type: Simple
- Output type: Prediction
- Dataset #: 1
- Trend type: None
- Transformation: Normal Score Transformation
- Approximation: DensitySkew
- Kernels: 4
- BaseDistribution: Student's t-distribution

Searching neighborhood

- Standard
- Neighbors to include: 5
- Include at least: 2
- Sector type: Four and 45 degree
- Major semiaxis: 37,444.9735554807
- Minor semiaxis: 37,444.9735554807
- Angle: 0

Variogram **Covariance**

- Number of lags: 12
- Lag size: 4,680.621694435087
- Nugget: 0.2918375624
- Measurement error %: 100

Model type **Stable**

- Parameter: 0.85390625
- Range: 37,444.9735554807
- Anisotropy: No
- Partial sill: 0.523464175044

